

Conservation Laws shape Dissipation

Riccardo Rao and Massimiliano Esposito

*Complex Systems and Statistical Mechanics, Physics and Materials Science
Research Unit, University of Luxembourg, L-1511 Luxembourg, G.D. Luxembourg*

(Dated: January 14, 2023)

Starting from the most general formulation of stochastic thermodynamics—*i.e.* a thermodynamically consistent nonautonomous stochastic dynamics describing systems in contact with several reservoirs—, we define a procedure to identify the conservative and the minimal set of nonconservative contributions in the entropy production. The former is expressed as the difference between changes caused by time-dependent drivings and a generalized potential difference. The latter is a sum over the minimal set of flux-force contributions controlling the dissipative flows across the system. When the system is initially prepared at equilibrium (*e.g.* by turning off drivings and forces), a finite-time detailed fluctuation theorem holds for the different contributions. Our approach relies on identifying the complete set of conserved quantities and can be viewed as the extension of the theory of generalized Gibbs ensembles to nonequilibrium situations.

PACS numbers: 02.50.Ga, 05.70.Ln.

I. INTRODUCTION

Stochastic Thermodynamics provides a rigorous formulation of nonequilibrium thermodynamics for open systems described by Markovian dynamics [1–4]. Thermodynamic quantities fluctuate and the first and second law of thermodynamics can be formulated along single stochastic trajectories. Most notably, entropy-production fluctuations exhibit a universal symmetry, called fluctuation theorem (FT). This latter implies, among other things, that the average entropy production (EP) is non-negative. Besides being conceptually new, this framework has been shown experimentally relevant in many different contexts [5]. It also provides a solid ground to analyze energy conversion [3, 6, 7], the cost of information processing [8–12], and speed–accuracy trade-offs [13, 14] in small systems operating far from equilibrium.

In stochastic thermodynamics, the dynamics is expressed in terms of Markovian rates describing transition probabilities per unit time between states. The thermodynamics, on the other hand, assigns conserved quantities to each system state (*e.g.* energy and particle number). This means that transitions among states entail an exchange of these conserved quantities between the system and the reservoirs. The core assumption providing the connection between dynamics and thermodynamics is local detailed balance. It states that the log ratio of each forward and backward transition rate corresponds to the entropy changes in the reservoirs caused by the exchange of the conserved quantities (divided by the Boltzmann constant). These changes are expressed as the product of the entropic intensive fields characterizing the reservoirs (*e.g.* inverse temperature, chemical potential divided by temperature) and the corresponding changes of conserved quantities in the reservoirs, in accordance to the fundamental relation of equilibrium thermodynamics in the entropy representation. Microscopically, the local detailed balance arises from the assumption that the reservoirs are at equilibrium [15].

In this paper, we ask a few simple questions which lie at the heart of nonequilibrium thermodynamics. We consider a system subject to time-dependent drivings—*i.e.* nonautonomous—and in contact with multiple reservoirs. What is the most

fundamental representation of the EP for such a system? In other words, how many independent nonconservative forces multiplied by their conjugated flux appear in the EP? Which thermodynamic potential is extremized by the dynamics in absence of driving when the forces are set to zero? How do generic time-dependent drivings affect the EP? Surprisingly, up to now, no systematic procedure exists to answer these questions. We provide one in this paper based on a systematic identification of conserved quantities. While some of them are obvious from the start (*e.g.* energy and particle number) the others are system specific and depend on the way in which reservoirs are coupled to the system and on the topology of the network of transitions.

The main outcome of our analysis is a rewriting of the EP, Eq. (60), which identifies three types of contributions: A driving contribution caused by the nonautonomous mechanisms, a change of a generalized Massieu potential, and a flow contribution made of a sum over a fundamental set of flux-force contributions. For autonomous systems relaxing to equilibrium—all forces must be zero—, the first and the third contributions vanish and the dynamics maximizes the potential. This amounts to a dynamical realization of the maximization of the Shannon entropy under the constraints of conserved quantities, which is commonly done by hand when deriving generalized Gibbs distributions. For (autonomous) steady-state dynamics, the first two contributions vanish and we recover the results of Ref. [16], showing that conservation laws reduce the number of forces created by the reservoirs. The key achievement of this paper is to demonstrate that conservation laws are essential to achieve a general and systematic treatment of stochastic thermodynamics.

Important results ensue. We show that system-specific conservation laws can cause the forces to depend on system quantities and not only on intensive fields. We derive the most general formulation of finite-time detailed FTs expressed in terms of measurable quantities. This result amounts to make use of conservation laws on the FT derived in Ref. [17]. We identify the minimal cost required for making a transformation from one system state to another one. In doing so we generalize to multiple reservoirs the nonequilibrium Landauer’s

principle derived in Refs. [18–20]. We also apply our method to four different models which reveal different implications of our theory.

This paper is organized as follows. In § II we derive an abstract formulation of stochastic thermodynamics. We then describe the procedure to identify all conserved quantities, which we use to rewrite the local detailed balance in terms of potential and (nonconservative) flow contributions. In § III we use the above decomposition to establish balance equations along stochastic trajectories, which allow us to formulate our finite-time detailed FT, § IV. In § V we discuss the ensemble average description of the EP decomposition and discuss the nonequilibrium Landauer’s principle. Three detailed applications conclude our analysis, § VI: in the first, § VIA, we describe a quantum point contact tightly coupled to a quantum dot; in § VIB we analyze a molecular motor; finally, we investigate a randomized grid in § VIC; In addition, we exemplify our theory throughout the paper using a double quantum dot.

II. EDGE LEVEL DESCRIPTIION

We here introduce continuous-time Markov jump processes, as well as a general formulation of stochastic thermodynamics. We then identify the conservative and nonconservative contributions of the local detailed balance.

A. Stochastic Dynamics

We consider an externally driven open system characterized by a discrete number of states, which we label by n . Transitions between pairs of states, $n \xleftarrow{v} m$, are denoted by directed edges, $e \equiv (nm, v)$. The index $v = 1, \dots$ labels different types of transitions between the same pair of states, e.g. transitions due to different reservoirs. The time evolution of the probability of finding the system in the state n , $p_n \equiv p_n(t)$, is governed by the master equation

$$d_t p_n = \sum_e D_e^n \langle J^e \rangle, \quad (1)$$

which is here written as a continuity equation. Indeed, the *incidence matrix* D ,

$$D_e^n \equiv \begin{cases} +1 & \text{if } \xrightarrow{e} n \\ -1 & \text{if } \xleftarrow{e} n \\ 0 & \text{otherwise} \end{cases}, \quad (2)$$

associates each edge to the pair of states that it connects. It thus encodes the topology of the network. On the graph identified by $\{n\}$ and $\{e\}$, it can be thought of as a (negative) divergence operator when acting on edge-space vectors—as in the master equation (1)—or as a gradient operator when acting on state-space vectors. The ensemble averaged edge probability currents,

$$\langle J^e \rangle \equiv \langle J_{nm}^v \rangle \equiv w_{nm}^v p_m, \quad (3)$$

index	label for	number
n	state	N_n
e	transition	N_e
$y \equiv (\chi, r)$	conserved quantity χ from reservoir r	$N_y = N_\chi N_r$
α	cycle	N_α
λ	conservation law and conserved quantity	N_λ
y_p	“potential” y	N_λ
y_f	“force” y	$N_y - N_\lambda$
ρ	symmetry	N_ρ
η	fundamental cycle	$N_\alpha - N_\rho$ $= N_y - N_\lambda$

TABLE I. Summary of the indices used throughout the paper and the object they label.

are expressed in terms of the transition rates, $\{w_{nm}^v \equiv w_e \equiv w_e(t)\}$, which describe the probability per unit time of transitioning from m to n via a transition of type v . For thermodynamic consistency, each transition $e \equiv (nm, v)$ with finite rate w_e has a corresponding backward transition $-e \equiv (mn, v)$ with a finite rate w_{-e} . The stochastic dynamics is assumed to be ergodic at any time.

Notation From now on, upper-lower indices and Einstein summation notation will be used: repeated upper-lower indices implies the summation over all the allowed values for those indices. The meaning of all the indices that will be used is summarized in Tab. I. Time derivatives are denoted by “ d_t ” or “ ∂_t ” whereas the overdot “ \cdot ” is reserved for rates of change of quantities that are not exact time derivatives. We also take the Boltzmann constant k_B equal to 1.

B. Stochastic Thermodynamics

Physically, each system state, n , is characterized by given values of some *system quantities*, $\{\chi_n\}$, for $\chi = 1, \dots, N_\chi$, which encompass the internal energy, E_n , and possibly additional ones, see Tab. II for some examples. These must be regarded as *conserved quantities*, as their change in the system is always balanced by an opposite change in the reservoirs. Indeed, when labeling the reservoirs with $\{r\}$, for $r = 1, \dots, N_r$, the balance equation for χ can be written as

$$\underbrace{\chi_n - \chi_m \equiv \chi_{n'} D_e^{n'}}_{\text{system}} = \sum_r \underbrace{Y_e^{(\chi, r)}}_{\text{reservoir } r}. \quad (4)$$

where $Y_e^{(\chi, r)}$ quantifies the flow of χ supplied by the reservoir r to the system along the transition e . For the purpose of our discussion, we introduce the index $y = (\chi, r)$, i.e. “*the conserved quantity χ exchanged with the reservoir r* ”, and define the matrix Y whose entries are $\{Y_e^y \equiv Y_e^{(\chi, r)}\}$. Enforcing microscopic reversibility, one concludes that $Y_e^y = -Y_{-e}^y$. As a first remark, more than one reservoir may be involved in each transition, see Fig. 1 and the application in § VIA. As a second remark, the conserved quantities may not be solely $\{\chi_n\}$, since additional ones may arise due to the topological properties of the system, as we will see in the next subsection.

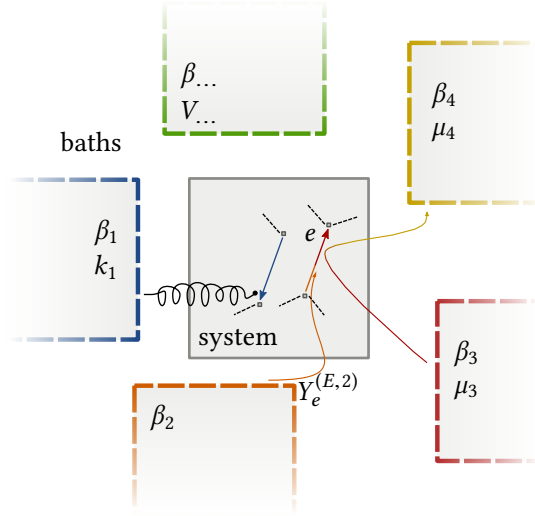


FIG. 1. Pictorial representation of a system coupled to several reservoirs. Transitions may involve more than one reservoir and exchange between reservoirs. Work producing reservoirs are also taken into account.

system quantity χ	intensive field $f_{(\chi,r)}$
energy, E_n	inverse temperature, β_r
particles number, N_n	chemical potential, $-\beta_r \mu_r$
charge, Q_n	electric potential, $-\beta_r V_r$
displacement, X_n	generic force, $-\beta_r k_r$
angle, θ_n	torque, $-\beta_r \tau_r$

TABLE II. Examples of system quantity–intensive field conjugated pairs in the entropy representation [21, § 2–3]. $\beta_r := 1/T_r$ denotes the inverse temperature of the reservoir. Since charges are carried by particles, the conjugated pair $(Q_n, -\beta_r V_r)$ is usually embedded in $(N_n, -\beta_r \mu_r)$, see e.g. Refs. [22, 23].

Each reservoir r is characterized by a set of *entropic intensive fields*, $\{f_{(\chi,r)}\}_{\chi=1,\dots,N_\chi}$, which are conjugated to the exchange of the system quantities $\{\chi_n\}$ [21, § 2–3]. A short list of χ – $f_{(\chi,r)}$ conjugated pairs is reported in Tab. II. The thermodynamic consistency of the stochastic dynamics is ensured by the *local detailed balance property*,

$$\ln \frac{w_e}{w_{-e}} = -f_y Y_e^y + S_n D_e^n. \quad (5)$$

It relates the log ratio of the forward and backward transition rates to the entropy change generated in the reservoirs, *i.e.* minus the entropy flow $\{-f_y Y_e^y\}$. The second term on the rhs is the internal entropy change occurring during the transition, since S_n denotes the internal entropy of the state n . This point is further evidenced when writing the entropy balance along a transition

$$\ln \frac{w_{nm}^y p_m}{w_{mn}^y p_n} = -\sum_r \left\{ \sum_\chi f_{(\chi,r)} Y_e^{(\chi,r)} \right\} + [S_n - \ln p_n] D_e^n, \quad (6)$$

which expresses the edge EP, the lhs, as the entropy change in each reservoir r plus the system entropy change, the rhs.

In the most general formulation, the internal entropy S_n , the conserved quantities $\{\chi_n\}$ (hence $\{Y_e^y\}$), and their conjugated fields $\{f_y\}$, may change in time. Physically, this modeling corresponds to two possible ways of controlling a system: either through $\{\chi_n\}$ or $\{S_n\}$ which characterize the system states, or through $\{f_y\}$ which characterize the properties of the reservoirs. Throughout the paper, we use the word “driving” to describe any of these time-dependent controls, while we refer to those systems that are not time-dependently driven as *autonomous*.

Example 1. Let us consider the system made of two single-level quantum dots (QD) depicted in Fig. 2a and presented in Ref. [24] as a physical implementation of a Maxwell Demon. The energy landscape and the network of transitions are shown in Figs. 2b and 2c, respectively. Electrons can enter empty dots from the reservoirs but cannot jump from one dot to the other. When the two dots are occupied, an interaction energy, u , arises.

Energy, E_n , and total number of electrons, N_n , characterize each system state:

$$\begin{aligned} E_{00} &= 0, & N_{00} &= 0, \\ E_{01} &= \epsilon_u, & N_{01} &= 1, \\ E_{10} &= \epsilon_d, & N_{10} &= 1, \\ E_{11} &= \epsilon_u + \epsilon_d + u, & N_{11} &= 2, \end{aligned} \quad (7)$$

where the first entry in n refers to the occupancy of the upper dot while the second to the lower. The entries of the matrix Y corresponding to the forward transitions are

$$Y = \begin{pmatrix} +1 & +2 & +3 & +4 & +5 & +6 \\ (E,1) & \epsilon_u & 0 & 0 & \epsilon_u + u & 0 & 0 \\ (N,1) & 1 & 0 & 0 & 1 & 0 & 0 \\ (E,2) & 0 & \epsilon_d & 0 & 0 & \epsilon_d + u & 0 \\ (N,2) & 0 & 1 & 0 & 0 & 1 & 0 \\ (E,3) & 0 & 0 & \epsilon_d & 0 & 0 & \epsilon_d + u \\ (N,3) & 0 & 0 & 1 & 0 & 0 & 1 \end{pmatrix}, \quad (8)$$

see Fig. 2c, whereas the entries related to backward transition are equal to the negative of the forward. For instance, along the first transition the system gains ϵ_u energy and 1 electron from the reservoir 1. The vector of entropic intensive fields is given by

$$\mathbf{f} = \begin{pmatrix} (E,1) & (N,1) & (E,2) & (N,2) & (E,3) & (N,3) \\ \beta_1 & -\beta_1 \mu_1 & \beta_2 & -\beta_2 \mu_2 & \beta_3 & -\beta_3 \mu_3 \end{pmatrix}. \quad (9)$$

Since the QDs and the electrons have no internal entropy, $S_n = 0, \forall n$, the local detailed balance property, Eq. (5), can be easily recovered from the product $-\mathbf{f} Y$. From a stochastic dynamics perspective, the detailed balance property arises when considering fermionic transition rates: $w_e = \Gamma_e (1 + \exp\{f_y Y_e^y\})^{-1}$ and $w_{-e} = \Gamma_e \exp\{f_y Y_e^y\} (1 + \exp\{f_y Y_e^y\})^{-1}$ for electrons entering and leaving the dot. \square

C. Network-Specific Conserved Quantities

We now define the procedure to identify the complete set of conserved quantities of a system. For this purpose, let

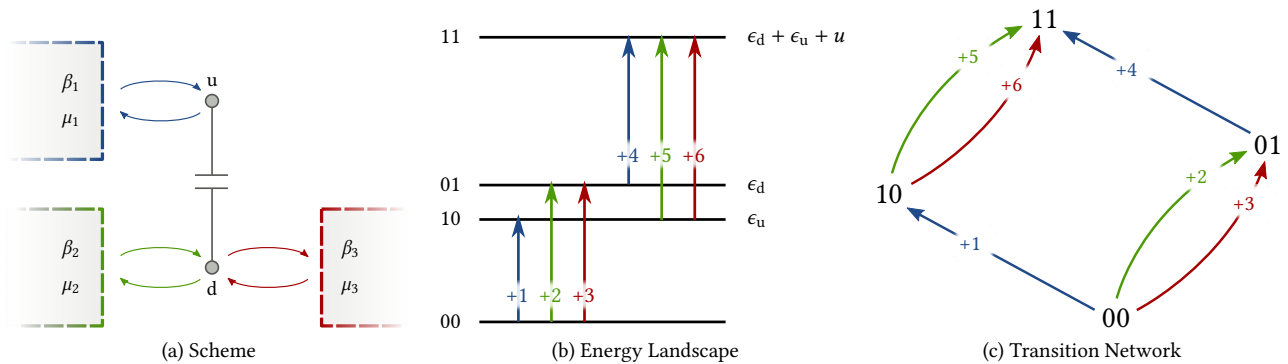


FIG. 2. Double QD coupled to three reservoirs and coupled with each other via a capacitor. Transitions related to the first reservoir are depicted in blue while those related to the second and third one by green and red, respectively. (a) Pictorial representation of the system. The upper dot u is coupled to the first reservoir, while the lower dot d is coupled to the second and third reservoir. The reservoirs exchange energy and electrons with the dots, which cannot host more than one electron. (b) Energy landscape of the dot. Importantly, when both dots are occupied, 11, a repulsive energy u adds to the occupied dots energies, ϵ_u and ϵ_d . (c) Transition network of the model.

$\{C_\alpha\}_{\alpha=1,\dots,N_\alpha \equiv \dim \ker D}$, be a basis of $\ker D$,

$$D_e^n C_\alpha^e = 0, \quad \forall n. \quad (10)$$

Since D is $\{-1, 0, 1\}$ -valued, $\{C_\alpha\}$ can always be chosen in such a way that their entries are $\{0, 1\}$ and at most one entry in each forward-backward transition pair is nonzero. In this representation, they can be interpreted as *cycles*, since its entries identify sets of transitions forming loops. In the examples, we will represent cycles using the set of forward transitions only, and negative entries denote transitions along the backward direction. We denote the matrix whose columns are $\{C_\alpha\}$ by $C \equiv \{C_\alpha^c\}$.

By multiplying the matrices Y and C , we obtain the M -matrix [16]:

$$M_\alpha^y := Y_e^y C_\alpha^e. \quad (11)$$

This fundamental matrix encodes the *physical topology* of the system. It describes the ways in which the conserved quantities $\{\chi_n\}$ are exchanged between the reservoirs across the system, as its entries quantify the influx of $\{y\}$ along each cycle, α . The physical topology is clearly build on top of the network topology encoded in C .

The bases of $\text{coker } M$, $\{\ell^\lambda\}_{\lambda=1,\dots,N_\lambda \equiv \dim \text{coker } M}$, identify the complete sets of conservation laws,

$$\ell_u^\lambda M_\alpha^y \equiv \ell_u^\lambda Y_e^y C_\alpha^e = 0, \quad \forall \alpha. \quad (12)$$

Indeed, the state variables $\{L^\lambda\}$ implicitly defined by

$$L_n^\lambda D_e^n \equiv \ell_y^\lambda Y_e^y \equiv \sum_r \left\{ \sum_\chi \ell_{(\chi, r)}^\lambda Y_e^{(\chi, r)} \right\} \quad (13)$$

are conserved quantities, since their changes along all cycles vanish [25], and the above equations can be interpreted as balance equations: the lhs identifies the change of $\{L^\lambda\}$ in the system, while the rhs expresses their change in the reservoirs. Importantly, the vector space spanned by the conserved quantities, $\{L^\lambda\}$, encompasses the system quantities $\{\chi_n\}$. They

correspond to $\ell_y^\chi \equiv \ell_{(\chi', r)}^\chi = \delta_{\chi'}^\chi$, so that the balance equations (4) are recovered. The remaining conservation laws arise from the interplay between the *specific* topology of the network, C , and its coupling with the reservoirs, Y , and we will refer to them as *nontrivial*. Only for these, the row vector ℓ may depend on time since M is a function of time, see Ex. 2 and the application in § VIA.

Variations in time of the system properties $\{\chi_n\}$ induce changes in the matrix M . If these changes cause a modification of the size of its cokernel, *i.e.* a change in the number of conserved quantities, we say that the physical topology was altered. We emphasize that these changes are not caused by changes in the network topology since this latter remains unaltered. An example of change of physical topology is given in the Ex. 2 and in the application in § VI C, while one of a changed network topology is briefly discussed in § VIB.

Example 2. We now come back to the two single-level QDs depicted in Fig. 2. An independent set of cycles of this network, Fig. 2c, is stacked in the matrix

$$C = \begin{pmatrix} 1 & 2 & 3 \\ +1 & \begin{pmatrix} 1 & 0 & 0 \\ 0 & 1 & 0 \\ -1 & -1 & 0 \\ -1 & 0 & 0 \end{pmatrix} \\ +2 & \\ +3 & \\ +4 & \\ +5 & \\ +6 & \end{pmatrix}, \quad (14)$$

and corresponds to the cycles depicted in Fig. 3. The negative entries denote transitions performed in the backward direction. The M -matrix readily follows from the product of Y and

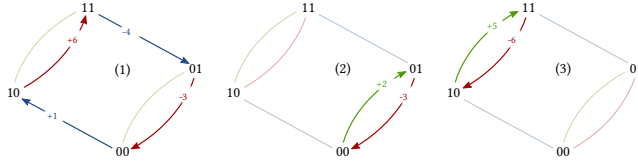


FIG. 3. The independent set of cycles corresponding to the columns of C in Eq. (14). The first corresponds to the sequence “electron in $u \rightarrow$ electron in $d \rightarrow$ electron out of $u \rightarrow$ electron out of d ”, in which the lower QD is populated by the third reservoir. The second and third cycle correspond to the flow of one electron from the second reservoir to the third one, when the upper QD is empty and filled, respectively.

the above matrix,

$$M = \begin{pmatrix} 1 & 2 & 3 \\ (E,1) & -u & 0 & 0 \\ (N,1) & 0 & 0 & 0 \\ (E,2) & 0 & \epsilon_d & \epsilon_d + u \\ (N,2) & 0 & 1 & 1 \\ (E,3) & u & -\epsilon_d & -\epsilon_d - u \\ (N,3) & 0 & -1 & -1 \end{pmatrix}. \quad (15)$$

Its cokernel is spanned by

$$\ell^E = \begin{pmatrix} (E,1) & (N,1) & (E,2) & (N,2) & (E,3) & (N,3) \\ 1 & 0 & 1 & 0 & 1 & 0 \end{pmatrix} \quad (16a)$$

$$\ell^u = \begin{pmatrix} (E,1) & (N,1) & (E,2) & (N,2) & (E,3) & (N,3) \\ 0 & 1 & 0 & 0 & 0 & 0 \end{pmatrix} \quad (16b)$$

$$\ell^d = \begin{pmatrix} (E,1) & (N,1) & (E,2) & (N,2) & (E,3) & (N,3) \\ 0 & 0 & 0 & 1 & 0 & 1 \end{pmatrix}. \quad (16c)$$

The first vector identifies the energy state variable, E_n ,

$$\ell^E Y = \begin{pmatrix} +1 & +2 & +3 & +4 & +5 & +6 \\ \epsilon_u & \epsilon_d & \epsilon_d & \epsilon_u + u & \epsilon_d + u & \epsilon_d + u \end{pmatrix} \equiv \{E_n D_e^n\}. \quad (17)$$

The other two, instead, give the occupancy of the upper and lower dots, N_n^u and N_n^d ,

$$\begin{aligned} \ell^u Y &= \begin{pmatrix} +1 & +2 & +3 & +4 & +5 & +6 \\ 1 & 0 & 0 & 1 & 0 & 0 \end{pmatrix} \equiv \{N_n^u D_e^n\}, \\ \ell^d Y &= \begin{pmatrix} +1 & +2 & +3 & +4 & +5 & +6 \\ 0 & 1 & 1 & 0 & 1 & 1 \end{pmatrix} \equiv \{N_n^d D_e^n\}. \end{aligned} \quad (18)$$

A posteriori, we see that these conservation laws arise from the fact that no electron transfer from one dot to the other is allowed. The total occupancy of the system, N_n , is recovered from the sum of the last two vectors. Despite ℓ^u and ℓ^d are nontrivial conservation laws, they do not depend on any system quantity, Eq. (7), [26].

Let us now imagine that the interaction energy between the two dots is switched off, *i.e.* $u \rightarrow 0$. Two conservation

laws emerge in addition to those in Eq. (16)

$$\ell^{(E,d)} = \begin{pmatrix} (E,1) & (N,1) & (E,2) & (N,2) & (E,3) & (N,3) \\ 0 & 0 & 1 & 0 & 1 & 0 \end{pmatrix} \quad (19a)$$

$$\ell^t = \begin{pmatrix} (E,1) & (N,1) & (E,2) & (N,2) & (E,3) & (N,3) \\ 0 & 0 & -1 & \epsilon_d & 0 & 0 \end{pmatrix}. \quad (19b)$$

The first is related to the upper–lower QD decoupling, as it corresponds to the conservation of energy of the lower dot

$$\ell^{(E,d)} Y = \begin{pmatrix} +1 & +2 & +3 & +4 & +5 & +6 \\ 0 & \epsilon_d & \epsilon_d & 0 & \epsilon_d & \epsilon_d \end{pmatrix} \equiv \{E_n^d D_e^n\}. \quad (20)$$

The conservation of energy in the upper dot is obtained as the difference between Eqs. (16a) and (19a), and it reads

$$\ell^{(E,u)} Y = \begin{pmatrix} +1 & +2 & +3 & +4 & +5 & +6 \\ \epsilon_u & 0 & 0 & \epsilon_u & 0 & 0 \end{pmatrix} \equiv \{E_n^u D_e^n\}. \quad (21)$$

The second one, Eq. (19b), arises from the tight coupling between the transport of energy and matter through the second dot. Since ℓ^t is in $\text{coker } Y$,

$$\ell^t Y = \begin{pmatrix} +1 & +2 & +3 & +4 & +5 & +6 \\ 0 & 0 & 0 & 0 & 0 & 0 \end{pmatrix} \equiv \{L_n^t D_e^n\}, \quad (22)$$

the conserved quantity L_n^t is a constant for all n , which can be chosen arbitrarily, see Remark 7. Notice the dependence on the system quantity ϵ_d of the nontrivial conservation law (19b). We thus showed that changes of system quantities (u in our case) can modify the properties of M , and hence the set of conservation laws—without changing the network topology. \square

D. Network-Specific Local Detailed Balance

We now make use of the conserved quantities, $\{Y_e^\lambda\}$, to separate the conservative contributions in the local detailed balance (5) from the nonconservative ones. To do so, we split the set $\{y\}$ into two groups: a “potential” one $\{y_p\}$, and an “force” one $\{y_f\}$. The first must be constructed with N_λ elements such that the matrix whose entries are $\{\ell_{y_p}^\lambda\}$ is nonsingular. We denote the entries of the inverse of the latter matrix by $\{\bar{\ell}_\lambda^{y_p}\}$. Crucially, since the rank of the matrix whose rows are $\{\ell^\lambda\}$ is N_λ , it is always possible to identify a set of $\{y_p\}$. However, it may not be unique and different sets have different physical interpretations, see Exs. 3 and 6 as well as the following sections. The second group, $\{y_f\}$, is constructed with the remaining $N_y - N_\lambda$ elements of $\{y\}$.

With the above prescription, we can write the entries $\{Y_e^{y_p}\}$ as functions of $\{Y_e^{y_f}\}$ and $\{L_n^\lambda\}$ by inverting $\{\ell_{y_p}^\lambda\}$ in Eq. (13),

$$Y_e^{y_p} = \bar{\ell}_\lambda^{y_p} L_n^\lambda D_e^n - \bar{\ell}_\lambda^{y_p} \ell_{y_f}^\lambda Y_e^{y_f}. \quad (23)$$

The local detailed balance (5) can thus be rewritten as

$$\ln \frac{w_e}{w_{-e}} = \phi_n D_e^n - \mathcal{F}_{y_f} Y_e^{y_f}. \quad (24)$$

The first contribution is conservative since it derives from the *potential*

$$\phi_n := S_n - F_\lambda L_n^\lambda, \quad (25)$$

where

$$F_\lambda := f_{y_p} \bar{\ell}_\lambda^{y_p} \quad (26)$$

is a linear combination of entropic intensive fields. Since ϕ_n is the entropy of the state n minus a linear combination of conserved quantities, it can be viewed as the Massieu potential of the state n . [We recall that Massieu potentials are the thermodynamic potentials of the entropy representation, see [21, § 5-4].] In contrast, the nonconservative *fundamental forces*,

$$\mathcal{F}_{y_f} := f_{y_f} - f_{y_p} \bar{\ell}_\lambda^{y_p} \ell_{y_f}^\lambda, \quad (27)$$

are caused by the presence of multiple reservoirs. Importantly, “fundamental” must be understood as a property of the set of these forces, since they are independent and in minimal number.

Remark 1. We saw that driving in the system quantities $\{\chi_n\}$, may induce changes in the physical topology, whereas the driving in the reservoir properties, $\{f_y\}$,—as well as in the entropy, S_n —is unable to do so. Accordingly, ϕ_n and $\{\mathcal{F}_{y_f}\}$, Eq. (24), change: the break of conservation laws entails the emergence of fundamental forces, and *vice versa* the creation of conservation laws destroys some fundamental forces and creates additional terms in ϕ_n , see Ex. 3.

Remark 2. Even in absence of topological changes, the form of ϕ_n and $\{\mathcal{F}_{y_f}\}$ may change in presence of driving. It is clear that ϕ_n changes when $\{\chi_n\}$, S_n , or $\{f_{y_p}\}$ change, see Eq. (25). Notice that since $\{f_{y_p}\}$ are entropic fields, they always depend on the inverse temperature of the reservoirs that they refer to, see Tab. II. Hence, whenever f_{y_f} is a field conjugated with the exchange of energy with one of the reservoirs in $\{y_p\}$ —*i.e.* an inverse temperature that appears in $\{f_{y_p}\}$ —, its changes will affect ϕ_n , too. Changes in the other f_{y_f} , leave ϕ_n unaltered. In turn, the fundamental forces depend on both $\{f_{y_p}\}$ and $\{f_{y_f}\}$, see Eq. (27). But in presence of nontrivial conservation laws, they may also depend on the system quantities $\{\chi_n\}$ via the vectors $\{\ell^\lambda\}$, see Ex. 3 and the application in § VIA.

The identification of ϕ_n and $\{\mathcal{F}_{y_f}\}$ and their relation with the local detailed balance, Eq. (24), is the key result of our paper and we summarize it in Fig. 4. The complete set of conservation laws played an essential role in this identification. In the following sections we will explore the various physical implications of Eq. (24).

Example 3. We now provide the expressions of ϕ_n and \mathcal{F}_{y_f} for the two single-level QDs depicted in Fig. 2a. Therefore, we split the set $\{y\}$ in $\{y_p\} = \{(E, 1), (N, 1), (N, 2)\}$ and $\{y_f\} = \{(E, 2), (E, 3), (N, 3)\}$. From Eq. (16) we see the validity of this splitting, as the matrix whose entries are $\{\ell_{y_p}^\lambda\}$ is an

identity matrix. The fields conjugated with the complete set of conservation laws, Eq. (26), are

$$F_E = \beta_1, \quad F_u = -\beta_1 \mu_1, \quad F_d = -\beta_2 \mu_2, \quad (28)$$

from which the Massieu potential of the state n follows

$$\phi_n = -\beta_1 E_n + \beta_1 \mu_1 N_n^u + \beta_2 \mu_2 N_n^d. \quad (29)$$

The fundamental forces are given by

$$\mathcal{F}_{(E, 2)} = \beta_2 - \beta_1, \quad (30a)$$

$$\mathcal{F}_{(E, 3)} = \beta_3 - \beta_1, \quad (30b)$$

$$\mathcal{F}_{(N, 3)} = \beta_2 \mu_2 - \beta_3 \mu_3. \quad (30c)$$

The first two forces rule the energy flowing from the first to the second and third reservoir, respectively, whereas the third force rules the electrons flowing from the second to the third reservoir.

Concerning the way the changes of ϕ_n and $\{\mathcal{F}_{y_f}\}$ are intertwined, we see that the former depends on β_1, μ_1, μ_2 , and β_2 , which arises from $f_{(N, 2)}$. Therefore, while the changes of $f_{(E, 3)} = \beta_3$ and $f_{(N, 3)} = -\beta_3 \mu_3$ only affect the forces, the changes of $f_{(E, 2)} = \beta_2$ affect both the forces and ϕ_n . Since the vectors of conservation laws (16) do not depend on $\{\chi_n\}$, see Ex. 2, the forces do not depend on $\{\chi_n\}$ either.

Alternatively, one may split the set $\{y\}$ in $\{y_p\} = \{(N, 1), (E, 2), (N, 3)\}$ and $\{y_f\} = \{(E, 1), (N, 2), (E, 3)\}$. With this choice, we obtain

$$\phi_n = -\beta_2 E_n + \beta_1 \mu_1 N_n^u + \beta_3 \mu_3 N_n^d, \quad (31)$$

and

$$\mathcal{F}_{(E, 1)} = \beta_1 - \beta_2, \quad (32a)$$

$$\mathcal{F}_{(N, 2)} = \beta_3 \mu_3 - \beta_2 \mu_2, \quad (32b)$$

$$\mathcal{F}_{(E, 3)} = \beta_3 - \beta_2. \quad (32c)$$

With respect to the previous decomposition, the interest here is shifted from the energy flow in the second reservoir, to that in the first reservoir, and the electrons flow from the third to the second reservoir.

Let us now imagine that the interaction energy u vanishes, as in the previous example. The five conservation laws that we consider are $E_n, E_n^d, N_n^u, N_n^d, L_n^t$, and we choose to split $\{y\}$ as $\{y_p\} = \{(E, 1), (N, 1), (E, 2), (N, 2), (E, 3)\}$ and $\{y_f\} = \{(N, 3)\}$. The potential follows

$$\phi'_n = -\beta_1 E_n + \beta_1 \mu_1 N_n^u + [\beta_2 \mu_2 - (\beta_2 - \beta_3) \epsilon_d] N_n^d - (\beta_3 - \beta_1) E_n^d - (\beta_3 - \beta_2) L_n^t. \quad (33)$$

whereas the only force is

$$\mathcal{F}'_{(N, 3)} = \beta_2 (\mu_2 - \epsilon_d) - \beta_3 (\mu_3 - \epsilon_d). \quad (34)$$

We see that the creation of two conservation laws destroyed two forces, Eqs. (30a) and (30b), whose expression can be spotted in the new potential, Eq. (33). Notice also how the emergence of the nontrivial conservation law (19b) makes the fundamental force dependent on the system quantity ϵ_d . \square

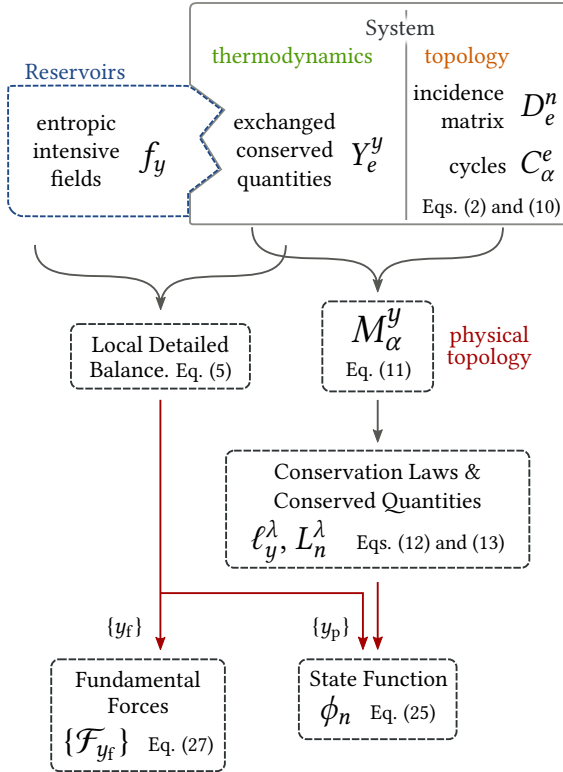


FIG. 4. Schematic representation of our local detailed balance decomposition, which we summarize as follows. On the one hand, the system is characterized by those system quantities which are exchanged with the reservoirs along transitions, as well as by the topological properties of its network of transitions. The former is accounted for by the matrix of exchanged conserved quantities Y , while the latter by the incidence matrix, D , Eq. (2), which determines the matrix of cycles, C , Eq. (10). These two matrices combined give the M -matrix, Eq. (11), which encodes the physical topology of the system and whose cokernel identifies the complete set of conservation laws and conserved quantities, Eq. (12) and (13). On the other hand, the reservoirs are characterized by entropic intensive fields, $\{f_y\}$, which combined with the matrix of exchanged conserved quantities, Y , gives the local detailed balanced, Eq. (5). Having identified all conservation laws, the variables y can be split into “potential” y , $\{y_p\}$, and “force” y , $\{y_f\}$. The first group identifies a Massieu potential for each state n , ϕ_n , Eqs. (25), while the second one identifies the fundamental forces, Eq. (27). These two set of thermodynamic quantities are thus combined in the local detailed balanced, (24).

E. Fundamental Cycles

We now show the conservative–nonconservative-forces decomposition of the local detailed balance in terms of cycle affinities.

The thermodynamic forces acting along cycles are referred to as *cycle affinities*. Using the local detailed balance (24), they read

$$\mathcal{A}_\alpha := C_\alpha^e \ln \frac{w_e}{w_{-e}} = -\mathcal{F}_{y_f} M_\alpha^{y_f}. \quad (35)$$

As observed in Ref. [16], different cycles may be connected to the same set of reservoirs, thus carrying the same cycle

affinity. These are regarded as *symmetries* and they correspond to bases of $\ker M$, $\{\psi_\rho\}_{\rho=1,\dots,N_\rho \equiv \dim \ker M}$,

$$M_\alpha^y \psi_\rho^\alpha = 0, \quad \forall y, \quad (36)$$

as its entries identify sets of cycles which, once completed, leave the state of the reservoirs unchanged, see Ex. 4 and the application in § VI C. As first derived in Ref. [16], the rank-nullity theorem applied to the matrix M allows us to relate the number of symmetries to the number of conservation laws

$$N_y - N_\lambda = N_\alpha - N_\rho. \quad (37)$$

Notice that, while the N_y and N_α are fixed for a given system, N_λ , and hence N_ρ , can change due to changes in the physical topology. From Eq. (37) we thus learn that for any broken (resp. created) conservation law, a symmetry must break (resp. be created), see Ex. 4.

The symmetries identified by Eq. (36) lead us to define $N_\eta := N_\alpha - N_\rho$ cycles, labeled by η , for which the entries of M , $\{M_\eta^y\}$, identify a maximal rank matrix. These cycles can be thought of as physically independent, since they cannot be combined to form cycles that leave the reservoirs unchanged upon completion. We refer to these cycles as *fundamental cycles*. As a result, the matrix whose entries are $\{M_\eta^{y_f}\}$ is square and nonsingular, see Note [27], and there is a one-to-one correspondence between fundamental forces, Eq. (27), and cycle affinities corresponding to fundamental cycles,

$$\mathcal{F}_{y_f} = -\mathcal{A}_\eta \bar{M}_{y_f}^\eta, \quad (38)$$

where $\{\bar{M}_{y_f}^\eta\}$ are the entries of the inverse matrix of that having $\{M_\eta^y\}$ as entries. We will refer to $\{\mathcal{A}_\eta\}$ as *fundamental affinities*. In terms of these latter, the local detailed balance, Eq. (24), reads

$$\ln \frac{w_e}{w_{-e}} = \phi_n D_e^n + \mathcal{A}_\eta \zeta_e^\eta. \quad (39)$$

where

$$\zeta_e^\eta := \bar{M}_{y_f}^\eta Y_e^{y_f} \quad (40)$$

quantifies the contribution of each transition e to the current along the fundamental cycle η as well as all those cycles which are physically dependent on η , see Ex. 4. Algebraically, the row vectors of ζ , $\{\zeta^\eta\}$, are dual to the physically independent cycles, $\{C_\eta\}$,

$$\zeta_e^\eta C_{\eta'}^e = \bar{M}_{y_f}^\eta Y_e^{y_f} C_{\eta'}^e = \bar{M}_{y_f}^\eta M_{\eta'}^{y_f} = \delta_{\eta'}^\eta. \quad (41)$$

An important remark is that our definition of set of fundamental cycles should not be confused with that constructed using spanning trees discussed in Ref. [28]. Eq. (39) is another important result of our paper, which expresses the conservative–nonconservative local detailed balance decomposition in terms of fundamental affinities. Importantly, the affinities $\{\mathcal{A}_\eta\}$ depend on time both via $\{f_y\}$ and $\{\chi_n\}$, where the latter originates from the M -matrix, Eq. (35). Differently from $\{\mathcal{F}_{y_f}\}$, they always have the dimension of an entropy.

Example 4. The two single-level QD, Fig. 2a, has no symmetries for $u \neq 0$, since its M -matrix, Eq. (15), has empty kernel. Its three cycle affinities, Eqs. (14) and (35), are thus fundamental and read

$$\mathcal{A}_1 = \beta_1 u - \beta_3 u, \quad (42a)$$

$$\mathcal{A}_2 = \beta_3(\epsilon_d - \mu_3) - \beta_2(\epsilon_d - \mu_2), \quad (42b)$$

$$\mathcal{A}_3 = \beta_3(\epsilon_d + u - \mu_3) - \beta_2(\epsilon_d + u - \mu_2), \quad (42c)$$

while the matrix relating fundamental cycles to edges, Eq. (40), is given by

$$\zeta_e^\eta = \begin{pmatrix} +1 & +2 & +3 & +4 & +5 & +6 \\ 1 & 0 & \epsilon_d & \epsilon_d & 0 & \epsilon_d + u & \epsilon_d + u \\ 0 & -\epsilon_d & -\epsilon_d - u & 0 & -\epsilon_d - u & -\epsilon_d - u & \\ 3 & 0 & \epsilon_d & \epsilon_d & 0 & \epsilon_d + u & \epsilon_d \end{pmatrix} \frac{1}{u}. \quad (43)$$

In sharp contrast with the fundamental forces, Eq. (30), the fundamental affinities, Eq. (42), depend both on the fields, Eq. (9), and the system quantities, Eq. (7).

As the interaction energy is turned off, two symmetries emerge:

$$\psi_1 = \begin{pmatrix} 1 & 2 & 3 \\ 1 & 0 & 0 \end{pmatrix} \quad (44a)$$

$$\psi_2 = \begin{pmatrix} 1 & 2 & 3 \\ 0 & 1 & -1 \end{pmatrix}, \quad (44b)$$

in agreement with the creation of two conservation laws, see Eqs. (19) and (37). They inform us that since the QDs are decoupled: (i) the cycle 1 does not produce changes in the reservoirs, *i.e.* its affinity is zero; (ii) the cycle 2 and 3 are physically dependent since the flow of electrons from the second to the third bath is the same with empty and filled upper dot. Choosing the third cycle as the fundamental one, its affinity reads

$$\mathcal{A}'_3 = \beta_2(\epsilon_d - \mu_2) - \beta_3(\epsilon_d - \mu_3). \quad (45)$$

whereas the matrix of cycle contributions, see Eq. (40) and Ex. 3, reads

$$\zeta_e^3 = \begin{pmatrix} +1 & +2 & +3 & +4 & +5 & +6 \\ 0 & 0 & -1 & 0 & 0 & -1 \end{pmatrix}. \quad (46)$$

Notice that both the transition +3—which belongs to the cycle 2—and +6—which belongs to the cycle 3—contribute to the current along the fundamental cycle 3. \square

F. Detailed-Balanced Networks

A dynamics is *detailed balanced* if at any stage the forces are zero

$$\mathcal{F}_{y_f} = f_{y_f} - f_{y_p} \ell_{\lambda}^{y_p} \ell_{y_f}^{\lambda} = 0, \quad (47)$$

or equivalently the affinities are zero—see Eq. (35). A driven detailed-balance dynamics implies that the driving must keep

the forces equal to zero at all times, while changing the potential ϕ_n . An autonomous detailed-balanced dynamics will always relax to an equilibrium distribution [29, 30]

$$p_n^{\text{eq}} = \exp \{ \phi_n - \Phi_{\text{eq}} \}, \quad (48)$$

defined by the detailed balance property: $w_{nm}^v p_m^{\text{eq}} = w_{mn}^v p_n^{\text{eq}}$, $\forall n, m, v$. The last term, Φ_{eq} , is the log of the partition function

$$\Phi_{\text{eq}} := \ln \{ \sum_m \exp \{ \phi_m \} \}, \quad (49)$$

and can be identified as an *equilibrium Massieu potential* [21, §§ 5-4 and 19-1].

Remark 3. One can transform a nondetailed-balance dynamics with the potential ϕ_n into a detailed-balanced dynamics with the same potential, if one can turn off the forces—set them to zero—without changing the potential. For isothermal system, this is always possible through an appropriate choice of $\{f_{y_f}\}$, Eq. (47). For nonisothermal systems, this is possible as long as: (i) there are no f_{y_f} that are inverse temperatures in $\{y_p\}$; (ii) if there are, their corresponding force \mathcal{F}_{y_f} vanish beforehand. Importantly, different local detailed balance decompositions involve different ϕ_n and $\{\mathcal{F}_{y_f}\}$ and the condition (ii) may be fulfilled in some decomposition while not in others, see next Example.

Example 5. From Eq. (30), we see that the two single-level QDs model of Fig. 2 is detailed balanced when $\beta_1 = \beta_2 = \beta_3$ and $\mu_2 = \mu_3$. In this case the Massieu potential of state n , Eq. (29), is given by

$$\phi_n = -\beta_1 \left(E_n - \mu_1 N_n^u - \mu_2 N_n^d \right). \quad (50)$$

The only element distinguishing the latter from that in Eq. (29) is the fact that $\beta_2 = \beta_1$, which arises from $\mathcal{F}_{(E,2)} = 0$. Therefore, a nondetailed-balanced dynamics described by the decomposition (29)–(30) can become detailed-balance without changing ϕ_n as long as $\mathcal{F}_{(E,2)} = 0$. The decomposition (31)–(32), instead, requires both $\mathcal{F}_{(E,1)}$ and $\mathcal{F}_{(E,3)}$ to be zero. \square

Remark 4. The equilibrium distribution, Eq. (48), can be obtained from a Maximum Entropy approach [31, 32]. Indeed, the distribution maximizing the entropy functional constrained by given values of the average conserved quantities $\{\langle L^\lambda \rangle = L^\lambda\}$,

$$S[p] = \sum_n p_n [S_n - \ln p_n] - a(\sum_n p_n - 1) - a_\lambda \left(\sum_n p_n L_n^\lambda - L^\lambda \right), \quad (51)$$

is given by

$$p_n^* = \exp \{ S_n - a_\lambda L_n^\lambda - a \}. \quad (52)$$

This is the equilibrium distribution, Eq. (48), when the Lagrange multipliers are given by $a = \Phi_{\text{eq}}$ and $a_\lambda = F_\lambda$, see Eq. (25) and (49).

III. TRAJECTORY LEVEL DESCRIPTION

We now scale our description to the level of trajectories. A stochastic *trajectory* of duration t , \mathbf{n}_t , is defined as a set of transitions $\{e_i\}$ sequentially occurring at times $\{t_i\}$ starting from n_0 at time t_0 . If not otherwise stated, the transitions index i runs from $i = 1$ to the last transition prior to time t , N_t , whereas the state at time $\tau \in [t_0, t]$ is denoted by n_τ . The values of S_n , $\{\chi_n\}$, and $\{f_y\}$ between time t_0 and an arbitrary time t are all encoded in the *protocol* π_τ , for $\tau \in [t_0, t]$.

We first derive the balance for the conserved quantities, Eq. (13). The conservative and nonconservative contributions identified at the level of single transitions via the local detailed balance, Eqs. (24) and (39), are then used to decompose the trajectory EP into its three fundamental contributions.

A. Balance of Conserved Quantities

Since the conserved quantities are state variables their change along a trajectory for a given protocol reads

$$\begin{aligned} \Delta L^\lambda[\mathbf{n}_t|\pi] &\equiv L_{n_t}^\lambda(t) - L_{n_0}^\lambda(t_0) \\ &= \int_{t_0}^t d\tau \left\{ \partial_\tau L_n^\lambda(\tau) \Big|_{n=n_\tau} + L_n^\lambda(\tau) D_e^n J^e(\tau) \right\}. \end{aligned} \quad (53)$$

The first term on the rhs accounts for the instantaneous changes due to the time-dependent driving, while the second accounts for the finite changes due to stochastic transitions, since

$$J^e(\tau) := \sum_i \delta_{e_i}^e \delta(\tau - t_i) \quad (54)$$

are the trajectory-dependent instantaneous currents at time τ . Using the edge-wise balance, Eq. (13), we can recast the above equation into

$$\Delta L^\lambda[\mathbf{n}_t|\pi] = \int_{t_0}^t d\tau \left\{ \partial_\tau L_n^\lambda(\tau) \Big|_{n=n_\tau} + \ell_y^\lambda(\tau) I^y(\tau) \right\}, \quad (55)$$

where

$$I^y(\tau) := Y_e^y(\tau) J^e(\tau), \quad (56)$$

quantify the instantaneous influx of y at time t .

B. Entropy Balance

The trajectory entropy balance is given by

$$\begin{aligned} \Sigma[\mathbf{n}_t|\pi] &= \int_{t_0}^t d\tau J^e(\tau) \ln \frac{w_e(\tau)}{w_{-e}(\tau)} - \ln \frac{p_{n_t}(t)}{p_{n_0}(t_0)} \\ &= \int_{t_0}^t d\tau f_y(\tau) Y_e^y(\tau) J^e(\tau) + \left[(s_{n_t} - s_{n_0}) - \ln \frac{p_{n_t}(t)}{p_{n_0}(t_0)} \right], \end{aligned} \quad (57)$$

As for the edge-wise balance, Eq. (6), the lhs is the EP, while the first and second term on the rhs are the entropy flow

	dynamics	v	$\Delta\Phi$	σ
autonomous	o			
NESS	o	o		
driven	detailed-balanced			o
autonomous	detailed-balanced	o		o

TABLE III. Entropy production for common processes. “o” denotes vanishing or negligible contribution, NESS is the acronym of *nonequilibrium steady state*.

and the entropy change of the system [28, 33]. Using our decomposition of the local detailed balance, Eq. (24), we can recast the latter equality into

$$\begin{aligned} \Sigma[\mathbf{n}_t|\pi] &= -\ln \frac{p_{n_t}(t)}{p_{n_0}(t_0)} \\ &+ \int_{t_0}^t d\tau \left\{ \phi_n(\tau) D_e^n J^e(\tau) - \mathcal{F}_{y_f}(\tau) I^{y_f}(\tau) \right\}. \end{aligned} \quad (58)$$

Since ϕ_n is a state variable, its variations along the trajectory can be written as

$$\begin{aligned} \Delta\phi[\mathbf{n}_t|\pi] &\equiv \phi_{n_t}(t) - \phi_{n_0}(0) \\ &= \int_{t_0}^t d\tau \left\{ \phi_n(\tau) D_e^n J^e(\tau) + \partial_\tau \phi_n(\tau) \Big|_{n=n_\tau} \right\}. \end{aligned} \quad (59)$$

By combining Eq. (58) with Eqs. (59)–(61), we can recast the trajectory EP in

$$\Sigma[\mathbf{n}_t|\pi] = v[\mathbf{n}_t|\pi] + \Delta\Phi[\mathbf{n}_t|\pi] + \sum_{y_f} \sigma_{y_f}[\mathbf{n}_t|\pi], \quad (60)$$

where

$$v[\mathbf{n}_t|\pi] := - \int_{t_0}^t d\tau \partial_\tau \phi_n(\tau) \Big|_{n=n_\tau}, \quad (61)$$

$$\sigma_{y_f}[\mathbf{n}_t|\pi] := - \int_{t_0}^t d\tau \mathcal{F}_{y_f}(\tau) I^{y_f}(\tau), \quad (62)$$

$$\Delta\Phi[\mathbf{n}_t|\pi] := \Phi_{n_t}(t) - \Phi_{n_0}(t_0), \quad (63)$$

with

$$\Phi_n := \phi_n - \ln p_n. \quad (64)$$

Eq. (60), is the major result of our paper. It shows the EP decomposed into a time-dependent driving contribution, a potential difference, and a minimal set of flux-force terms. The first term only arises in presence of time-dependent driving. It quantifies the entropy dissipated when ϕ_n is modified and we refer to it as the *driving contribution*. The second term is entirely conservative as it involves a difference between the final and initial *stochastic Massieu potential*, Eq. (64). The last terms are nonconservative and prevent the systems from reaching equilibrium. Each $\sigma_{y_f}[\mathbf{n}_t|\pi]$ quantifies the entropy produced by the flow of $\{y_f\}$, and we refer to them as *flow contributions*.

To develop more physical intuition of each single term, we now discuss them separately and consider some specific

cases. When writing the rate of driving contribution explicitly, Eq. (61), one obtains

$$-\partial_\tau \phi_n = -\partial_\tau S_n + \partial_\tau F_\lambda L_n^\lambda + F_\lambda \partial_\tau L_n^\lambda. \quad (65)$$

When all $\{\ell^\lambda\}$ are independent from system quantities, the terms, $\{\partial_\tau F_\lambda L_{\lambda,n}\}$, account for the entropy dissipated during the manipulation of the intensive fields $\{y_p\}$, Eq. (26). In contrast, $\{F_\lambda \partial_\tau L_{\lambda,n}\}$ and $-\partial_\tau S_n$ characterize the dissipation due to the direct manipulation of the system quantities. The changes of those f_{y_f} that are not fields conjugated with the exchange of energy with a reservoir in $\{y_p\}$ do not contribute to $v[\mathbf{n}_t|\pi]$, see Remarks 2 and 3.

For autonomous networks, the EP becomes

$$\Sigma[\mathbf{n}_t] = \Delta\Phi[\mathbf{n}_t] - \mathcal{F}_{y_f} \mathcal{I}^{y_f}[\mathbf{n}_t]. \quad (66)$$

where

$$\mathcal{I}^{y_f}[\mathbf{n}_t] := \int_{t_0}^t d\tau \mathcal{I}^{y_f}(\tau), \quad (67)$$

are the integrated currents of $\{y_f\}$ along the trajectory. The difference between the final and initial stochastic Massieu potential captures the dissipation due to changes of the internal state of the system. For finite-dimensional autonomous networks, it is typically subextensive in time and negligible with respect to the nonconservative terms for long trajectories

$$\Sigma[\mathbf{n}_t] \xrightarrow{t \rightarrow \infty} -\mathcal{F}_{y_f} \mathcal{I}^{y_f}[\mathbf{n}_t]. \quad (68)$$

The nonconservative flow contributions, Eqs. (62) and (68), quantify the dissipation due to the flow of conserved quantities across the network. Finally, for autonomous detailed-balanced systems, the nonconservative terms vanish, in agreement with the fact that these systems exhibit no net flows, and the EP becomes

$$\Sigma[\mathbf{n}_t] = \Delta\Phi[\mathbf{n}_t]. \quad (69)$$

Table III summarizes the contributions of the EP for these common processes.

Remark 5. It may occur that the driving protocol causes a change of the physical topology, which consequently alters the EP decomposition, see Remark 1 and Exs. 2 and 3. The trajectory must be thus decomposed into subtrajectories characterized by the same physical-topology properties. For each of these, our decomposition (60) applies.

Remark 6. The contributions of the EP in Eq. (60) depend on the choice of $\{y_p\}$ and $\{y_f\}$. When aiming at quantifying the dissipation of a physical system, some choices may be more convenient than others depending on the experimental apparatus, see next Example. This freedom can be thought of as a gauge of the EP. In the long time limit, it only affects the flow contributions and it can be understood as a particular case of the gauge freedoms discussed in Refs. [34, 35], which hinge on graph-theoretical arguments.

Example 6. For the sake of illustration let us assume that the system energy, $E_n(t)$, the chemical potential of the second reservoir, $\mu_2(t)$, and the temperature of the third one, $\beta_3(t)$, are controlled in time, in our favorite model of two single-level QDs. According to the expressions of ϕ_n and $\{\mathcal{F}_{y_f}\}$ derived in Ex. 3, we can distinguish two driving contributions of the EP, Eqs. (61) and (65):

$$v[\mathbf{n}_t|\pi] = v_E[\mathbf{n}_t|\pi] + v_{(N,2)}[\mathbf{n}_t|\pi], \quad (70)$$

where the first term,

$$v_E[\mathbf{n}_t|\pi] := \beta_1 \int_{t_0}^t d\tau \partial_\tau E_n(\tau)|_{n_\tau}, \quad (71)$$

is usually referred to as mechanical work in stochastic thermodynamics (up to β_1), while the second,

$$v_{(N,2)}[\mathbf{n}_t|\pi] := -\beta_2 \int_{t_0}^t d\tau \partial_\tau \mu_2(\tau) N_{n_\tau}^d, \quad (72)$$

is the entropy dissipated due to the change of the chemical potential of the second reservoir. The flow contributions, Eq. (62), are instead given by

$$\sigma_{(E,2)}[\mathbf{n}_t|\pi] = -\mathcal{F}_{(E,2)} \int_{t_0}^t d\tau I_{(E,2)}(\tau), \quad (73a)$$

$$\sigma_{(E,3)}[\mathbf{n}_t|\pi] = -\int_{t_0}^t d\tau \mathcal{F}_{(E,3)}(\tau) I_{(E,3)}(\tau), \quad (73b)$$

$$\sigma_{(N,3)}[\mathbf{n}_t|\pi] = -\int_{t_0}^t d\tau \mathcal{F}_{(N,3)}(\tau) I_{(N,3)}(\tau), \quad (73c)$$

where, the forces are given in Eq. (30), while the instantaneous currents of y_f are given by

$$I_{(E,2)} = \epsilon_d [J^{+2} - J^{-2}] + (\epsilon_d + u) [J^{+5} - J^{-5}], \quad (74a)$$

$$I_{(E,3)} = \epsilon_d [J^{+3} - J^{-3}] + (\epsilon_d + u) [J^{+6} - J^{-6}], \quad (74b)$$

$$I_{(N,3)} = J^{+3} - J^{-3} + J^{+6} - J^{-6}. \quad (74c)$$

We thus see that the first and the second flow contribution, Eqs. (73a) and (73b), quantify the dissipation due to the energy flow in the second and third reservoir, respectively. Analogously, the third contribution, Eq. (73c), characterizes the EP due to the flow of electrons in the third reservoir. The total EP of the system is thus the sum of the terms in Eqs. (70) and (73) plus a difference of stochastic Massieu potential, Eqs. (29) and (64). We notice that the change in time of β_3 is accounted for by the second and third flows, Eqs. (73b) and (73c), while not by a driving contribution, as β_3 does not contribute to ϕ_n , Eq. (29).

It is worth noting that, from an experimental point of view, the driving contribution demands information on the states of the trajectory. Instead, the flow contributions require the measurement of the energy flow in the second and third reservoir and the electron flow in the third. Let us now compare the above decomposition with that based on a different choice of $\{y_p, y_f\}$, e.g. the second one made in Ex. (3). In this case the driving contribution reads,

$$v[\mathbf{n}_t|\pi] = v_E[\mathbf{n}_t|\pi] + v_{(E,3)}[\mathbf{n}_t|\pi] \quad (75)$$

where

$$v_{(E,3)}[\mathbf{n}_t|\pi] := -\mu_3 \int_{t_0}^t d\tau \partial_\tau \beta_3(\tau) N_{n_\tau}^d. \quad (76)$$

The flow contributions read as in Eq. (73) with forces given in Eq. (32) and other expressions for the currents. Now, the measurement of the energy flow in the first and third reservoir, as well as the electron flow in the second reservoir, are required to quantify these terms in experiments.

To make the difference between the two choices even sharper, one can easily see that if the only quantity changing in time is μ_2 , the driving contribution of the second choice vanishes while that of the first does not. Therefore, depending on the physical system and the experimental apparatus, one choice may be more convenient than another when it comes to estimating the dissipation. \square

Remark 7. The driving contribution v and the nonequilibrium Massieu potential Φ_n are defined up to a gauge. This is evidenced when transforming the state variables $\{L^\lambda\}$ according to

$$L_n^\lambda(t) \rightarrow U_\lambda^\lambda L_n^{\lambda'}(t) + u^\lambda 1_n, \quad (77)$$

where $\{U_\lambda^\lambda\}$ identify a nonsingular matrix, $\{u^\lambda\}$ are finite coefficients, and $\{1_n\}$ a vector whose entries are 1. The first term can be considered as a basis change of $\text{coker } M$,

$$\ell_y^\lambda \rightarrow U_\lambda^\lambda \ell_y^{\lambda'}, \quad (78)$$

while the second as a *reference shift* of L^λ . Under the transformation (78), the fields (26) transform as

$$F_\lambda(t) \rightarrow F_{\lambda'}(t) \overline{U}_\lambda^{\lambda'}, \quad (79)$$

where $U_\lambda^{\lambda'} \overline{U}_{\lambda''} = \overline{U}_\lambda^{\lambda'} U_{\lambda''}^\lambda = \delta_{\lambda''}^{\lambda'}$, so that scalar products are preserved. As a consequence, the stochastic Massieu potential, Eq. (64), and the rate of driving contribution, Eq. (65), transform as

$$\begin{aligned} \Phi_n(t) &\rightarrow \Phi_n(t) - \mathfrak{f}(t) 1_n \\ -\partial_t \phi_n(t) &\rightarrow -\partial_t \phi_n(t) + \partial_t \mathfrak{f}(t) 1_n, \end{aligned} \quad (80)$$

where

$$\mathfrak{f}(t) := F_{\lambda'}(t) \overline{U}_\lambda^{\lambda'} u^\lambda. \quad (81)$$

Crucially, neither the local detailed balance (24) nor the EP (105) are affected, as the physical process is not changed. Also, if only a basis change is considered, $\{u^\lambda = 0\}$, then $\mathfrak{f}(t) = 0$, and both Φ_n and v are left unchanged. Finally, for cyclic protocols, it is easily shown that the driving work over a period is unchanged, since the gauge term $\mathfrak{f}(t)$ is nonfluctuating.

The above gauge is akin to that affecting the potential–work connection and which led to several debates, see Ref. [36] and references therein. The problem is rooted in what is experimentally measured, as different experimental set-ups constrain to different gauge choices [36]. We presented a general formulation of the gauge issue, by considering reference shifts of any conserved quantity, and not only of energy.

Fundamental Cycles

An equivalent decomposition of the EP, Eq. (57), can be achieved using the potential–affinities decomposition of the local detailed balance, Eq. (39):

$$\Sigma[\mathbf{n}_t|\pi] = v[\mathbf{n}_t|\pi] + \Delta\Phi[\mathbf{n}_t|\pi] + \sum_\eta \gamma_\eta[\mathbf{n}_t|\pi]. \quad (82)$$

Here,

$$\gamma_\eta[\mathbf{n}_t|\pi] := \int_{t_0}^t d\tau \mathcal{A}_\eta(\tau) \zeta_{\eta,e} J^e(\tau), \quad (83)$$

quantify the dissipation along the fundamental cycles, as $\{\zeta_{\eta,e} J^e(\tau)\}_{\eta=1,\dots,N_\eta}$ are the corresponding instantaneous currents, Eq. (40). For autonomous networks, the EP becomes

$$\Sigma[\mathbf{n}_t] = \Delta\Phi[\mathbf{n}_t] + \mathcal{A}_\eta \mathcal{Z}^\eta[\mathbf{n}_t] \quad (84)$$

where

$$\mathcal{Z}^\eta[\mathbf{n}_t] := \int_{t_0}^t d\tau \zeta_e^\eta J^e(\tau) \quad (85)$$

measure the total circulation along $\{\eta\}$. In general, Eq. (82) should not be considered as a graph-theoretical cyclic–cocyclic decomposition as in Ref. [37], since it is constructed using the physical topology of the system.

Example 7. For the scenario described in the previous example, Ex. 6, the flow contributions along fundamental cycles (83) read

$$\gamma_1[\mathbf{n}_t|\pi] = \int_{t_0}^t d\tau \mathcal{A}_1(\tau) \zeta_{1,e} J^e(\tau) \quad (86a)$$

$$\gamma_2[\mathbf{n}_t|\pi] = \int_{t_0}^t d\tau \mathcal{A}_2(\tau) \zeta_{2,e} J^e(\tau) \quad (86b)$$

$$\gamma_3[\mathbf{n}_t|\pi] = \int_{t_0}^t d\tau \mathcal{A}_3(\tau) \zeta_{3,e} J^e(\tau), \quad (86c)$$

where the affinities are given in Eq. (42) and the cycle–edge coupling matrix ζ in Eq. (43). Concerning their physical interpretation, the first contribution corresponds to the flow of energy from the third reservoir to the first, while the latter two to the entropy dissipated when transferring electrons from the second reservoir to the third with empty and filled upper dot, respectively. \square

IV. FINITE-TIME DETAILED FLUCTUATION THEOREM

The driving and flow contributions of the EP, Eq. (60), satisfy a finite-time detailed FT. We consider a *forward* (resp. *backward*) process characterized by the following properties:

1. The system is initially prepared at equilibrium, Eq. (48), which is identified by the potential $\phi_n(0)$ (resp. $\phi_n(t)$). It corresponds to the protocol state π_i (resp. π_f), in which all fundamental affinities vanish.

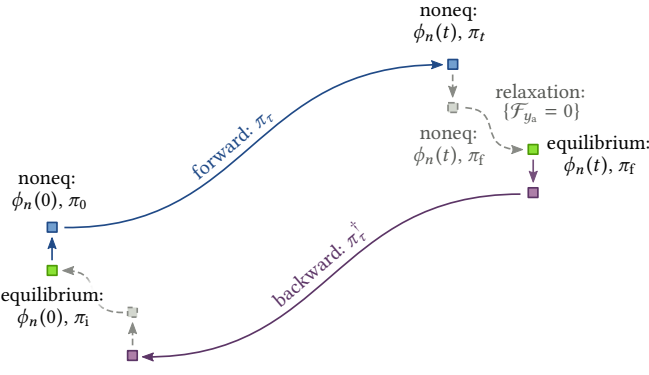


FIG. 5. Schematic representation of the forward and backward processes. The forward process starts at equilibrium, which corresponds to the initial protocol state π_i . At time 0, the protocol is switched on, $\pi_i \rightarrow \pi_0$, and the system evolves driven by π_τ until time t , when the protocol is switched off, $\pi_t \rightarrow \pi_f$. Importantly, the initial and final switches must not change the initial and final potential $\phi_n(0)$ and $\phi_n(t)$. Effectively, all the forces \mathcal{F}_{y_f} whose field f_{y_f} is conjugated with the exchange of energy with one reservoirs in $\{y_p\}$ must be vanishing for π_0 and π_t , see Remark 3. The backward process starts at the equilibrium defined by π_f and evolves according to the time-reversed protocol: $\pi_f \rightarrow \pi_0^\dagger - \pi_\tau^\dagger - \pi_t^\dagger \rightarrow \pi_i$. The relaxation to the equilibrium initial condition of the backward process that follows the switching off of forward protocol is irrelevant for the FT.

2. The driving protocol of the forward process, π_τ , (resp. of the backward process, $\pi_\tau^\dagger := \pi_{t-\tau}$), is arbitrary between $[0, t]$ except at the boundaries 0 and t , where π_0 and π_t must be such that the instantaneous switch from π_i to π_0 (resp. from π_f to π_t) leaves $\phi_n(0)$ (resp. $\phi_n(t)$) invariant, see Fig. 5.

The *finite-time detailed FT* states that the forward and backward process are related by

$$\frac{P_t(v, \{\sigma_{y_f}\})}{P_t^\dagger(-v, \{-\sigma_{y_f}\})} = \exp \left\{ v + \sum_{y_f} \sigma_{y_f} + \Delta\Phi_{\text{eq}} \right\}, \quad (87)$$

where $P_t(v, \{\sigma_{y_f}\})$ is the probability of observing a driving contribution to the EP v and flow ones $\{\sigma_{y_f}\}$ along the forward process. Instead, $P_t^\dagger(-v, \{-\sigma_{y_f}\})$ is the probability of observing a driving contribution equal to $-v$ and flow ones $\{-\sigma_{y_f}\}$ along the backward process. The difference of equilibrium Massieu potentials

$$\Delta\Phi_{\text{eq}} = \Phi_{\text{eq}_f} - \Phi_{\text{eq}_i}. \quad (88)$$

refers to the equilibrium distributions ruled by $\phi_n(t)$ and $\phi_n(0)$. When marginalizing with respect to the probability distribution of the backward process, the integral FT ensues

$$\langle \exp \left\{ -v - \sum_{y_f} \sigma_{y_f} \right\} \rangle = \exp \left\{ \Delta\Phi_{\text{eq}} \right\}. \quad (89)$$

We prove Eq. (87) in App. A using a generating function technique which is new to our knowledge.

To provide a physical interpretation of the argument of the exponential on the rhs of (87), let us observe that once the

protocol is switched off, $\pi_t \rightarrow \pi_f$, all fundamental forces vanish and the system relaxes to the equilibrium initial condition of the backward process. During the relaxation, neither v nor $\{\sigma_{y_f}\}$ evolve and the EP is equal to $\Phi_{\text{eq}_f} - \Phi_{\text{eq}_t}$, Eq. (69). Therefore, the argument of the exponential can be interpreted as the dissipation of the fictitious composite process “forward process + relaxation to equilibrium”.

For protocols keeping the potential ϕ_n constant, *viz.* $v = 0$, the FT (87) reads

$$\frac{P_t(\{\sigma_{y_f}\})}{P_t^\dagger(\{-\sigma_{y_f}\})} = \exp \left\{ \sum_{y_f} \sigma_{y_f} \right\}, \quad (90)$$

Notice that those flow contributions corresponding to f_{y_f} that are fields related to the exchange of energy with reservoirs in $\{y_p\}$ must vanish at all time for the condition 2 to be fulfilled. Yet a more specific case is that of autonomous protocols, for which the above FT becomes

$$\frac{P_t(\{\mathcal{I}^{y_f}\})}{P_t(\{-\mathcal{I}^{y_f}\})} = \exp \left\{ -\mathcal{F}_{y_f} \mathcal{I}^{y_f} \right\}, \quad (91)$$

written in terms of integrated currents of $\{y_f\}$, Eq. (67). Notice that since nothing distinguishes the forward process from the backward, the lhs is the ratio of the same probability distribution but at opposite values of $\{\mathcal{I}^{y_f}\}$, see application in § VI B.

Eq. (87) builds on the FT first derived in Ref. [17], which is recovered when solely accounting for nontrivial conservation laws, $\{\chi_n\}$. In this case, the number of forces increases (they are not fundamental anymore) and the number of conservation laws that appear in the Massieu potential is decreased. This has two crucial consequences: (i) the equilibrium distribution becomes a particular case of Eq. (48), since it is obtained by imposing additional forces to vanish; (ii) a part of the driving EP becomes a flow contribution, and—as one can check by comparing the two formulations of the FT—the requirement 2 is always satisfied. Finally, the Jarzynski–Crooks-like FTs [38, 39] are recovered for vanishing fundamental forces, *i.e.* in detailed-balanced systems,

$$\frac{P_t(v)}{P_t^\dagger(-v)} = \exp \left\{ v + \Delta\Phi_{\text{eq}} \right\}. \quad (92)$$

Remark 8. As we discussed in Eq. (65), the driving contribution consists of several subcontributions, one for each time-dependent parameter appearing in ϕ_n . We formulated the finite-time FT (87) for the whole v , but it can be equivalently expressed for the single subcontributions, see next Example.

Example 8. We now illustrate the conditions under which our FT applies to the coupled QD, Fig. 2. The process must start from equilibrium, Eq. (48): all forces vanish and the potential is given in Eq. (50). As the protocol is switched on, it must leave the fields appearing in ϕ_n , Eq. (29), $(\beta_1, \beta_2 (= \beta_1), \mu_1, \text{ and } \mu_2)$ unchanged, but all the others can be set to arbitrary values. Subsequently, all fields and system quantities can change controlled by π_τ for $\tau \in [0, t]$. At time t , the force in Eq. (30a) must be turned off, so that when the protocol is switched off—or equivalently the backward protocol is switched on—,

$\phi_n(t)$ does not change. When the above force vanishes at all times, one can formulate FTs like those in Eqs. (90) and (91).

To simplify the application of the FT let us consider the conditions described in Ex. 6, with the further simplification that all temperatures are equal and constant: only the E_n and μ_2 change in time. Since $\beta_2 = \beta_1$ at all times, condition 2 is satisfied and an application of Eq. (87) gives us

$$\frac{P_t(v_E, v_{(N,2)}, \sigma_{(N,3)})}{P_t^*(-v_E, -v_{(N,2)}, -\sigma_{(N,3)})} = \exp \{v_E + v_{(N,2)} + \sigma_{(N,3)} + \Delta\Phi_{\text{eq}}\}, \quad (93)$$

where the different contributions involved are given in Eqs. (71), (72), and (73c). \square

FT for Flow Contributions along Fundamental Cycles

In terms of the probability $P_t(v, \{\gamma_\eta\})$ of observing v driving contribution and $\{\gamma_\eta\}$ flow contributions along the fundamental cycles, the above FT reads

$$\frac{P_t(v, \{\gamma_\eta\})}{P_t^*(-v, \{-\gamma_\eta\})} = \exp \{v + \sum_\eta \gamma_\eta + \Delta\Phi_{\text{eq}}\}. \quad (94)$$

Its proof is discussed in App. A. Notice that, in the same way the condition 2 imposes that some forces must be vanishing at time 0 and t , see Fig. 5, here some combination of fundamental affinities must vanish. These combinations are readily identified using the relationship between $\{\mathcal{F}_{y_f}\}$ and $\{\mathcal{A}_\eta\}$, Eq. (38), see Ex. (9). For those autonomous processes in which the above condition is fulfilled at all times, one can express the FT for the integrated currents along fundamental cycles, Eq. (85),

$$\frac{P_t(\{\mathcal{Z}^\eta\})}{P_t(\{-\mathcal{Z}^\eta\})} = \exp \{\mathcal{A}_\eta \mathcal{Z}^\eta\}, \quad (95)$$

see Eq. (91).

Differently from all previous finite-time detailed FTs characterizing the dissipation along cycles, see e.g. [40], it involves the minimal set of fundamental ones. In the long time limit, we recover the steady-state FT derived in Ref. [16], which is in turn a refined version of the steady-state FT for Schnakenberg cycle currents formulated in Ref. [41].

Example 9. We saw in the previous example that the force $\mathcal{F}_{(E,2)}$, Eq. (30a), must be zero at time 0 and t for the FT (87) and at all times for the FTs (90) and (91). Using Eq. (38) in combination with the inverse of the submatrix of (15) whose entries are $\{M_\eta^{y_f}\}$,

$$\bar{M} = \frac{1}{2} \begin{pmatrix} (E,2) & (E,3) & (N,3) \\ 1 & 1 & 0 \\ -1 & 0 & -\epsilon_d - u \\ 1 & 0 & \epsilon_d \end{pmatrix} \frac{1}{u}, \quad (96)$$

we conclude that the above requirement becomes

$$\mathcal{A}_1 - \mathcal{A}_2 + \mathcal{A}_3 = 0, \quad (97)$$

in terms of fundamental affinities, Eq. (42). \square

V. ENSEMBLE AVERAGE LEVEL DESCRIPTION

We now present our results at the ensemble average level and derive a general formulation of the Nonequilibrium Landauer's Principle.

A. Balance of Conserved Quantities

Using the master equation (1) and the edge-wise balance (13), the balance equation for the average rates of changes of conserved quantities reads

$$d_t \left[\sum_n L_n^\lambda p_n \right] \equiv d_t \langle L^\lambda \rangle = \langle \dot{L}^\lambda \rangle + \ell_y^\lambda \langle I^y \rangle, \quad (98)$$

where

$$\langle \dot{L}^\lambda \rangle := \sum_n \partial_t L_n^\lambda p_n \quad (99)$$

is the average change due to the driving,

$$\langle I^y \rangle := Y_e^y \langle J^e \rangle \quad (100)$$

is the average currents of y , see Eqs. (3) and (56), and

$$\ell_y^\lambda \langle I^y \rangle \equiv \sum_r \left\{ \sum_\chi \ell_{(\chi,r)}^\lambda Y_e^{(\chi,r)} \langle J^e \rangle \right\}. \quad (101)$$

accounts for the average flow of the conserved quantities in the reservoirs. Obviously, the balances (98) can also be obtained by averaging the trajectory balances (55) along all stochastic trajectories.

B. Entropy Balance

In contrast to conserved quantities, entropy is not conserved. The EP rate measures this nonconservation and is always non-negative

$$\langle \dot{\Sigma} \rangle \equiv \sum_{n,m,v} w_{nm}^v p_m \ln \frac{w_{nm}^v p_m}{w_{mn}^v p_n} \geq 0. \quad (102)$$

The EP decomposition in driving, conservative and flow contributions at the ensemble level, can be obtained by averaging Eq. (60). Alternatively, one can rewrite Eq. (102) as

$$\langle \dot{\Sigma} \rangle = -f_y \langle I^y \rangle + [S_n - \ln p_n] D_e^n \langle J^e \rangle, \quad (103)$$

where we used the local detailed balance property (5) and the definition of average physical current (100). The first term is the average rate of entropy flow, while the second is the rate of change of the average system entropy. Using the splitting of the set $\{y\}$ explained in § II, the physical currents of $\{y_p\}$ can be expressed as

$$\langle I^{y_p} \rangle = \bar{\ell}_\lambda^{y_p} \left[d_t \langle L^\lambda \rangle - \langle \dot{L}^\lambda \rangle - \ell_{y_f}^\lambda \langle I^{y_f} \rangle \right], \quad (104)$$

where we partially inverted Eq. (98). When combined with Eq. (103), the EP rate can be written as

$$\langle \dot{\Sigma} \rangle = \langle \dot{v} \rangle + d_t \langle \Phi \rangle + \sum_{y_f} \langle \dot{\sigma}_{y_f} \rangle, \quad (105)$$

where $\langle \dot{v} \rangle = -\sum_n \partial_t \phi_n p_n$ is the driving contribution, $\langle \dot{\sigma}_{y_f} \rangle = -\mathcal{F}_{y_f} \langle I_{y_f} \rangle$ the flow contributions, and

$$\langle \Phi \rangle = \sum_n p_n \Phi_n \quad (106)$$

the *nonequilibrium Massieu potential*.

C. Nonequilibrium Massieu potential

In detailed-balanced systems, the nonequilibrium Massieu potential takes its maximum value at equilibrium, Eq. (48), where it becomes the equilibrium Massieu potential, Eq. (49). Indeed,

$$\Phi_{\text{eq}} - \langle \Phi \rangle = \langle \Phi_{\text{eq}} - \Phi \rangle = \mathcal{D}(p \| p^{\text{eq}}) \geq 0, \quad (107)$$

where

$$\mathcal{D}(p \| p^{\text{eq}}) := \sum_n p_n \ln \frac{p_n}{p_n^{\text{eq}}} \quad (108)$$

is the relative entropy between the nonequilibrium distribution and the equilibrium one which quantifies the distance from equilibrium.

Remark 9. For autonomous detailed-balanced networks, the difference of equilibrium and nonequilibrium initial Massieu potential, Eq. (107), gives the average dissipation during the relaxation to equilibrium, $\langle \Sigma \rangle = \mathcal{D}(p(t_0) \| p_{\text{eq}}) \geq 0$. This shows how the MaxEnt principle mentioned in Remark 4 is embedded in the stochastic thermodynamic description (see also Ref. [42]).

D. Nonequilibrium Landauer's Principle

We now express Eq. (105) in terms of a well defined equilibrium distribution, obtained by turning off the forces without modifying the potential ϕ_n . We already discussed that this procedure is always well defined for isothermal systems but requires more care for nonisothermal systems, see Remark 3. Combining Eqs. (105) and (107), one finds that

$$\langle \dot{\Sigma} \rangle = \langle \dot{v}_{\text{irr}} \rangle - d_t \mathcal{D}(p \| p^{\text{eq}}) + \sum_{y_f} \langle \dot{\sigma}_{y_f} \rangle, \quad (109)$$

where we introduced the average *irreversible driving contribution*

$$\langle \dot{v}_{\text{irr}} \rangle := \langle \dot{v} \rangle + d_t \Phi_{\text{eq}}. \quad (110)$$

Notice that the above contribution is not affected by the gauge discussed in Remark 7. Integrating Eq. (109) over time we get

$$\langle v_{\text{irr}} \rangle + \sum_{y_f} \langle \sigma_{y_f} \rangle = \Delta \mathcal{D}(p \| p_{\text{eq}}) + \langle \Sigma \rangle. \quad (111)$$

This relation generalizes the nonequilibrium Landauer's principle, which is typically derived for driven detailed-balance systems, $\langle \sigma_{y_f} \rangle = 0$, [20]—see also Refs. [18, 19, 42]—, and which is used as the basis to study thermodynamics of information processing [11]. It shows that not only driving but

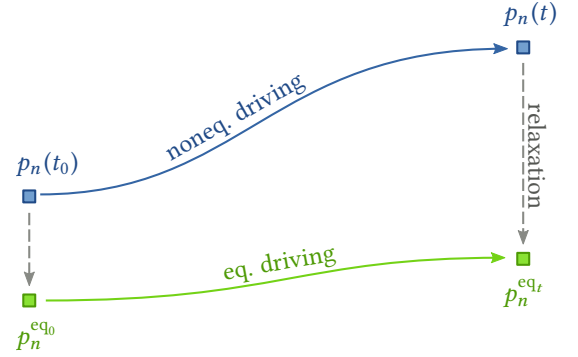


FIG. 6. Pictorial representation of the transformation between two nonequilibrium probability distributions. The protocol must leave the potential ϕ_n unchanged upon turning off of the forces, Remark 3, at all times. The nonequilibrium transformation (blue line) is compared with the equilibrium one (green line), which is obtained by turning off the forces, shutting down the driving and letting the system relax (dashed gray lines) at each time.

also flow EP must be consumed to move a system away from equilibrium, as depicted in Fig. 6, and that the minimal cost for doing so is precisely measured by the change in relative entropy. For driven detailed-balanced protocols connecting two equilibrium states, we recover the classical result that $\langle \dot{v}_{\text{irr}} \rangle = \langle \Sigma \rangle \geq 0$.

VI. APPLICATIONS

We here illustrate our formalism and main results on three more systems: a QD coupled to a quantum point contact, a molecular motor and a randomized grid.

A. QD coupled to a QPC

Here, we consider a simplified description of a two levels QD coupled to a thermal reservoir and a quantum point contact (QPC), Fig. 7. For a more detailed analysis of this class of systems we refer to Ref. [43]. The interest of this model lies in the transition triggered by the QPC, which involves the interaction with more than one thermal reservoir.

The two states of the QD, l for “low” and h for “high”, are characterized by different energies but the same number of electrons

$$E_l = 0, \quad E_h = \epsilon, \quad N_l = 1, \quad N_h = 1. \quad (112)$$

The transition between these states can occur following either a phononic interaction with the first reservoir, ± 1 , or following electron tunneling from the second to the third reservoir, ± 2 . Along the latter transition, an electron with energy $u + \epsilon$ leaves the second reservoir and enters the third with energy u . The

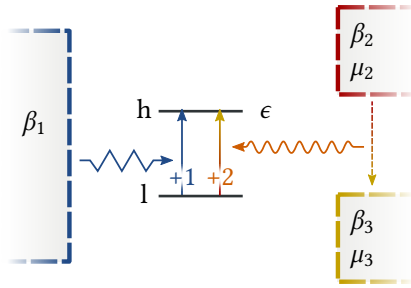


FIG. 7. Model of QD coupled with a thermal reservoir and a pair of particle reservoirs modeling a QPC. The electron can jump to the excited state following either a phononic interaction with the first reservoir or an interaction with the QPC. The latter involves an electron current from the second to the third reservoir.

matrix of exchanged conserved quantities, Y , thus reads

$$Y = \begin{pmatrix} (E, 1) & +1 & +2 \\ (E, 2) & \epsilon & 0 \\ (E, 2) & 0 & u + \epsilon \\ (N, 2) & 0 & 1 \\ (E, 3) & 0 & -u \\ (N, 3) & 0 & -1 \end{pmatrix}. \quad (113)$$

while the vector of intensive fields is

$$\mathbf{f} = \begin{pmatrix} (E, 1) & (E, 2) & (N, 2) & (E, 3) & (N, 3) \\ \beta_1 & \beta_2 & -\beta_2\mu_2 & \beta_3 & -\beta_3\mu_3 \end{pmatrix}. \quad (114)$$

The nontrivial local detailed balance property for the second transition follows from $-\mathbf{f}Y$, and reads

$$\ln \frac{w_+}{w_-} = -\beta_2(u + \epsilon - \mu_2) + \beta_3(u - \mu_3). \quad (115)$$

The M -matrix,

$$M = \begin{pmatrix} (E, 1) & 1 \\ (E, 2) & \epsilon \\ (E, 2) & -u - \epsilon \\ (N, 2) & -1 \\ (E, 3) & u \\ (N, 3) & 1 \end{pmatrix}, \quad (116)$$

follows from the product of Y , Eq. (113), and the matrix of cycles,

$$C = \begin{pmatrix} +1 \\ +2 \end{pmatrix} \begin{pmatrix} 1 \\ -1 \end{pmatrix}. \quad (117)$$

Its four-dimensional cokernel is spanned by

$$\ell^E = \begin{pmatrix} (E, 1) & (E, 2) & (N, 2) & (E, 3) & (N, 3) \\ 1 & 1 & 0 & 1 & 0 \end{pmatrix}, \quad (118a)$$

$$\ell^N = \begin{pmatrix} (E, 1) & (E, 2) & (N, 2) & (E, 3) & (N, 3) \\ 0 & 0 & 1 & 0 & 1 \end{pmatrix}, \quad (118b)$$

$$\ell^3 = \begin{pmatrix} (E, 1) & (E, 2) & (N, 2) & (E, 3) & (N, 3) \\ 0 & 1 & -u - \epsilon & 0 & 0 \end{pmatrix}, \quad (118c)$$

$$\ell^4 = \begin{pmatrix} (E, 1) & (E, 2) & (N, 2) & (E, 3) & (N, 3) \\ 0 & 0 & u & 1 & 0 \end{pmatrix}. \quad (118d)$$

The first two conservation laws are clearly the energy and the number of particles, Eq. (112), since $\ell^E Y = (\epsilon, \epsilon)$ and $\ell^N Y = (0, 0)$, while the other two to other constants, since $\ell^3 Y = \ell^4 Y = (0, 0)$. Mindful of the gauge freedom described in Remark 7 we can set the conserved quantities related to ℓ^N , ℓ^3 , and ℓ^4 to zero. When $(E, 1)$ is set as “force” y , the field related to the energy conservation law

$$F_E = [(\epsilon + u - \mu_2)\beta_2 - (u - \mu_3)\beta_3] / \epsilon, \quad (119)$$

determine the values of the nonequilibrium Massieu potential, $\phi_n = -F_E E_n$. Concerning the nonconservative contributions, the fundamental force and the fundamental affinity read

$$\mathcal{F}_{(E, 1)} = \beta_1 - F_E = -\epsilon \mathcal{A}_1. \quad (120)$$

Due to the emergence of nontrivial conservation laws, Eqs. (118c) and (118d), the fundamental force depends on a system quantity. In detailed balance dynamics, $\mathcal{F}_{(E, 1)} = 0$, and we readily recover $\phi_n = -\beta_1 E_n$.

B. Molecular Motor

Our thermodynamic description is also applicable to biological systems, as we now show on a molecular motor moving on a one-dimensional space, see Refs. [44, 45]. The presence of a work producing reservoir distinguishes this model from those described so far.

The motor conformations and transitions are described in Fig. 8. It can step against a mechanical force k thanks to the chemical force produced by the hydrolysis of ATP into ADP, which are exchanged with reservoirs at chemical potential μ_{ATP} and μ_{ADP} . We label each state of the process by $n = (m, x)$, while each transition by e_x , where $e \in \{1, 2, 3, 4, 5, 6, 7\}$ refers to the transitions at a given position $x \in \mathbb{Z}$. The system quantities are the internal energy, $E_n = \epsilon_m$, the total number of ATP plus ADP molecules attached to the motor, $N_n = N_m$, and the position, $X_n = xl$ where l is the size of a step. Importantly, each internal state is characterized by an internal entropy $S_n = s_m$.

The matrix of exchanged conserved quantities for the transitions at given position x is written as

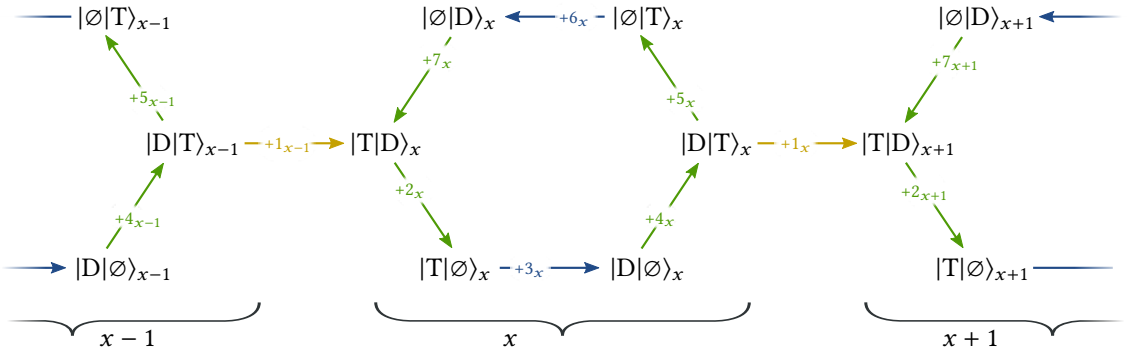


FIG. 8. Network of transitions describing the chemomechanical stepping of the motor, where x denotes the generic position along the stepping support. The molecular motor has six internal conformations distinguished by the state of the trailing, $|\cdot|$, and leading, $|\cdot\rangle$, motor foot: ATP-bound (T), ADP-bound (D), or unbound (\emptyset). Yellow arrows denote stepping transitions, $\{+1_x \equiv |D|T\rangle_x \rightarrow |T|D\rangle_{x+1}\}$, along which the mechanical force k acts (positive value drive the system toward increasing x). Internal transitions may entail the exchange of ATP and ADP molecules with particle reservoirs (green arrows) or the hydrolysis of ATP into ADP (blue arrows). The latter only exchange energy with the thermal reservoir at inverse temperature β .

$$Y_x = \begin{pmatrix} (E) & +1_x & +2_x & +3_x & +4_x & +5_x & +6_x & +7_x \\ (N, ATP) & \epsilon_{TD} - \epsilon_{DT} & \epsilon_{T\emptyset} - \epsilon_{TD} & \epsilon_{D\emptyset} - \epsilon_{T\emptyset} & \epsilon_{DT} - \epsilon_{D\emptyset} & \epsilon_{\emptyset T} - \epsilon_{DT} & \epsilon_{\emptyset D} - \epsilon_{\emptyset T} & \epsilon_{TD} - \epsilon_{\emptyset D} \\ (N, ADP) & 0 & 0 & 0 & 1 & 0 & 0 & 1 \\ (X) & 0 & -1 & 0 & 0 & -1 & 0 & 0 \\ & l & 0 & 0 & 0 & 0 & 0 & 0 \end{pmatrix}, \quad (121)$$

whereas the full matrix reads $Y = (\dots \ Y_{x-1} \ Y_x \ Y_{x+1} \ \dots)$. On the other side, the row vector of intensive variables is given by

$$\mathbf{f} = \begin{pmatrix} (E) & (N, ATP) & (N, ADP) & (X) \\ \beta & -\beta\mu_{ATP} & -\beta\mu_{ADP} & -\beta k \end{pmatrix}. \quad (122)$$

Differently from all previous cases, the local detailed balance of the step transitions involves the *work producing reservoir*, $(X, -\beta k)$,

$$\ln \frac{w_{+1_x}}{w_{-1_x}} = -\beta [(\epsilon_{TD} - \epsilon_{DT}) - kl] + (s_{TD} - s_{DT}). \quad (123)$$

Notice that the interpretation of the first term as minus entropy flow still holds: $q_{+1_x} \equiv (\epsilon_{TD} - \epsilon_{DT}) - kl$, since the last term is minus the work that the mechanical force exerts on the system along the step [46, 47].

It is easily shown that the subnetwork at given x contains exactly one cycle c_x ,

$$C_x = \begin{pmatrix} c_x \\ +1_x & 0 \\ +2_x & 1 \\ +3_x & 1 \\ +4_x & 1 \\ +5_x & 1 \\ +6_x & 1 \\ +7_x & 1 \end{pmatrix}, \quad (124)$$

which entails the intake of two ATP molecules and the release

of two ADP ones

$$M_x := Y_x C_x = \begin{pmatrix} c_x \\ (E) & 0 \\ (N, ATP) & 2 \\ (N, ADP) & -2 \\ (X) & 0 \end{pmatrix}, \quad (125)$$

irrespective of the position x . The full M -matrix has thus an infinite-number of columns equal to Eq. (125), and its three-dimensional cokernel is spanned by

$$\ell^E = \begin{pmatrix} (E) & (N, ATP) & (N, ADP) & (X) \\ 1 & 0 & 0 & 0 \end{pmatrix} \quad (126a)$$

$$\ell^N = \begin{pmatrix} (E) & (N, ATP) & (N, ADP) & (X) \\ 0 & 1 & 1 & 0 \end{pmatrix} \quad (126b)$$

$$\ell^X = \begin{pmatrix} (E) & (N, ATP) & (N, ADP) & (X) \\ 0 & 0 & 0 & 1 \end{pmatrix}, \quad (126c)$$

which clearly corresponds to the three system quantities, E_n , N_n , and X_n , respectively. As far as the symmetries are concerned, the intersection between its infinite-dimensional column vector space and its (infinite-dimensional) kernel is one-dimensional, in agreement with the observation that all cycles $\{c_x\}$ are physically dependent on one. In other words, there is an infinity of symmetries and all cycles carry the same cycle affinity

$$\mathcal{A} = 2\beta(\mu_{ATP} - \mu_{ADP}), \quad (127)$$

which is thus regarded as the fundamental affinity.

To illustrate our EP decomposition, we use $\{(E), (N, \text{ADP}), (X)\}$ as set of y_p , while leaving (N, ATP) as y_f . Guided by Eqs. (25) and (26), the potential reads

$$\phi_n = \omega_n + \beta k X_n, \quad (128)$$

where

$$\omega_n := S_n - \beta E_n + \beta \mu_{\text{ADP}} N_n, \quad (129)$$

is the Massieu potential corresponding to the grand potential. The fundamental affinities, Eq. (27), consist solely of

$$\mathcal{F}_{(N, \text{ATP})} = \beta(\mu_{\text{ADP}} - \mu_{\text{ATP}}). \quad (130)$$

The EP along a stochastic trajectory with autonomous protocol, Eq. (60), is

$$\Sigma[\mathbf{n}_t] = \beta(\mu_{\text{ATP}} - \mu_{\text{ADP}}) \mathcal{I}_{\text{ATP}}[\mathbf{n}_t] + \Delta\Phi[\mathbf{n}_t], \quad (131)$$

where

$$\begin{aligned} \mathcal{I}_{\text{ATP}}[\mathbf{n}_t] &:= \int_{t_0}^t d\tau Y_e^{(N, \text{ATP})} J^e(\tau) \\ &= \sum_{x=-\infty}^{\infty} \int_{t_0}^t d\tau [J^{+4_x}(\tau) - J^{-4_x}(\tau) + J^{+7_x}(\tau) - J^{-7_x}(\tau)] \end{aligned} \quad (132)$$

is the total number of ATP molecules flowing into the system, while Φ is the stochastic Massieu potential related to (128), Eq. (64). Since there is only one fundamental force, the EP in terms of fundamental affinities reads exactly as Eq. (131).

To illustrate the finite-time detailed FT, let us imagine a system with a finite number of positions $x = 1, \dots, N_x$. The potential (128) thus defines a physical equilibrium state, Eq. (48), achieved when the force is turned off: $\mu_{\text{ATP}} = \mu_{\text{ADP}}$. At time 0, the autonomous protocol with $\mu_{\text{ATP}} \neq \mu_{\text{ADP}}$ (but with the same μ_{ADP} as at equilibrium) is switched on and the system moves far from equilibrium. Notice that any switch of μ_{ATP} leaves ϕ_n unaltered, Eq. (128), and the process can be stopped at any time t . Hence, the probability of observing the intake of \mathcal{I}_{ATP} ATP molecules up to time t satisfies

$$\frac{P_t(\mathcal{I}_{\text{ATP}})}{P_t(-\mathcal{I}_{\text{ATP}})} = \exp \{ \beta(\mu_{\text{ATP}} - \mu_{\text{ADP}}) \mathcal{I}_{\text{ATP}} \}, \quad (133)$$

see Eq. (91).

To formulate a FT which explicitly counts the number of steps, we have to make a step backward and regard the conservative term $\beta k l$ in the local detailed balance, Eq. (123), as an additional force term, rather than as a conservative term. Under this condition the EP can be recast into

$$\Sigma[\mathbf{n}_t] = \beta(\mu_{\text{ATP}} - \mu_{\text{ADP}}) \mathcal{I}_{\text{ATP}}[\mathbf{n}_t] + \beta k \mathcal{X}[\mathbf{n}_t] + \Delta\Omega[\mathbf{n}_t], \quad (134)$$

where

$$\Omega_n = \omega_n - \ln p_n \quad (135)$$

is the stochastic Massieu potential corresponding to Eq. (129), while

$$\mathcal{X}[\mathbf{n}_t] := X_{n_t} - X_{n_0} \quad (136)$$

the total distance traveled by the motor. If the system is initially prepared in the grandcanonical equilibrium state—achieved by turning off both the external force k and the fundamental force $\mathcal{F}_{(N, \text{ATP})}$ —the FT reads

$$\frac{P_t(\mathcal{I}_{\text{ATP}}, \mathcal{X})}{P_t(-\mathcal{I}_{\text{ATP}}, -\mathcal{X})} = \exp \{ \beta(\mu_{\text{ATP}} - \mu_{\text{ADP}}) \mathcal{I}_{\text{ATP}} + \beta k \mathcal{X} \}. \quad (137)$$

Here, both μ_{ATP} and k must be turned on at time 0.

Tightly coupled model As an example of change of network topology, we now consider the tightly coupled description in which the transitions $\{5, 6, 7\}$ are absent, and the network becomes a one-dimensional chain of states. Since there are no cycles the whole row space of Y spans the conservation laws, which can thus be written as

$$\ell^E = \begin{pmatrix} (E) & (N, \text{ATP}) & (N, \text{ADP}) & (X) \\ 1 & 0 & 0 & 0 \end{pmatrix} \quad (138a)$$

$$\ell^{\text{ATP}} = \begin{pmatrix} (E) & (N, \text{ATP}) & (N, \text{ADP}) & (X) \\ 0 & 1 & 0 & 0 \end{pmatrix} \quad (138b)$$

$$\ell^{\text{ADP}} = \begin{pmatrix} (E) & (N, \text{ATP}) & (N, \text{ADP}) & (X) \\ 0 & 0 & 1 & 0 \end{pmatrix} \quad (138c)$$

$$\ell^X = \begin{pmatrix} (E) & (N, \text{ATP}) & (N, \text{ADP}) & (X) \\ 0 & 0 & 0 & 1 \end{pmatrix}, \quad (138d)$$

With respect to the previous model, the number of ATP and ADP molecules are separately conserved quantities, Eqs. (138b) and (138c). The set of fundamental forces is empty while the potential reads

$$\phi_n = S_n - \beta E_n + \beta \mu_{\text{ATP}} N_n^{\text{ATP}} + \beta \mu_{\text{ADP}} N_n^{\text{ADP}} + \beta k X_n, \quad (139)$$

thus making the dissipation equal to

$$\Sigma[\mathbf{n}_t] = \Delta\Phi[\mathbf{n}_t]. \quad (140)$$

In summary, the change of network topology achieved by removing transitions leading to cycles, prevents the reservoirs from creating forces. The potential will be thus described with the maximum amount of conserved quantities, one for each y .

Alternative Description An alternative description of the chemomechanical process is obtained when periodic boundary conditions are imposed, Fig. 9. One additional cycle is created,

$$C = \begin{pmatrix} c & a \\ +1 & \begin{pmatrix} 0 & 1 \\ 1 & 1 \end{pmatrix} \\ +2 & \begin{pmatrix} 1 & 1 \\ 1 & 1 \end{pmatrix} \\ +3 & \begin{pmatrix} 1 & 1 \\ 1 & 1 \end{pmatrix} \\ +4 & \begin{pmatrix} 1 & 1 \\ 1 & 1 \end{pmatrix} \\ +5 & \begin{pmatrix} 1 & 0 \\ 1 & 0 \end{pmatrix} \\ +6 & \begin{pmatrix} 1 & 0 \\ 1 & 0 \end{pmatrix} \\ +7 & \begin{pmatrix} 1 & 0 \\ 1 & 0 \end{pmatrix} \end{pmatrix}, \quad (141)$$

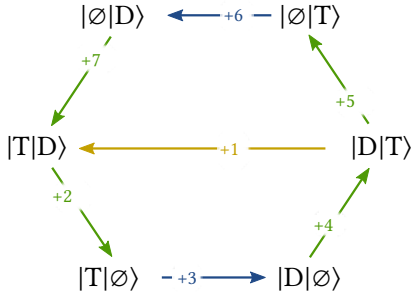


FIG. 9. Alternative description of the chemomechanical stepping process in Fig. 8. The kinetics and thermodynamics of the internal transitions is unchanged, while the step transitions reset the internal motor state.

cf. Eq. (124), and the M-matrix now reads

$$M := \begin{pmatrix} (E) & c & a \\ (N, ATP) & 0 & 0 \\ (N, ADP) & 2 & 1 \\ (X) & -2 & -1 \\ & 0 & l \end{pmatrix}, \quad (142)$$

As a consequence, the spatial conservation law, (126c), is lost and the nonequilibrium Massieu potential becomes ω_n , Eqs. (129) and (135). However, the set of fundamental forces gains one element,

$$\mathcal{F}_{(X)} = -\beta k, \quad (143)$$

which is conjugated to the traveled distance:

$$\begin{aligned} \mathcal{X}[\mathbf{n}_t] &:= \int_{t_0}^t d\tau Y_e^{(X)} J^e(\tau) \\ &= l \int_{t_0}^t d\tau [J^{+1_x}(\tau) - J^{-1_x}(\tau)]. \end{aligned} \quad (144)$$

Hence, the expression of the EP and the formulation of the finite-time detailed FT read as in Eqs. (134) and (137), respectively.

In conclusion, the periodic boundary condition can be viewed as a change of network topology in which one conservation law is destroyed and a fundamental force is created.

C. Randomized Grid

As a final illustration, we consider an abstract two-dimensional grid of states, $n = (x, z)$ for $x, z = 1, \dots, N$, coupled to random force fields. This system illustrate a class of models for which a systematic procedure for characterizing the thermodynamic behavior becomes essential. The states are characterized by a spatial coordinate $X_n = a_x x + a_z z$, and jumps are only allowed between nearest neighbors: $x \rightarrow x \pm 1$ or $z \rightarrow z \pm 1$. The system is isothermal and each transition is ruled by a force $f_{(X, r)} = -\beta k_r$, which is initially drawn randomly from a set of N_r reservoirs. The Y -matrix relating

transitions to reservoirs is given by

$$Y_e^r = \begin{cases} \pm a_x & \text{if } e = x \xrightarrow{r} x \pm 1 \\ \pm a_z & \text{if } e = z \xrightarrow{r} z \pm 1 \\ 0 & \text{otherwise} \end{cases}. \quad (145)$$

i.e. if e is triggered by the work producing reservoir r , then Y_e^r is equal to $\pm a_x$ or $\pm a_z$ depending on the direction of the transition.

As an example, we consider the 3×3 grid coupled to 5 reservoirs depicted in Fig. 10. We omit to report the matrices Y and C as they can be easily inferred from the picture and Eq. (145), and move on to the M -matrix, which reads

$$M = (X, 1) \begin{pmatrix} 1 & 2 & 3 & 4 \\ a_x & -a_x & 0 & a_x \\ 0 & a_x & a_z - a_x & -a_z \\ 0 & 0 & -a_z & 0 \\ -a_z & 0 & 0 & 0 \\ a_z - a_x & 0 & a_x & a_z - a_x \end{pmatrix}. \quad (146)$$

Its one-dimensional cokernel is spanned by the vector

$$\ell^X = \begin{pmatrix} (X, 1) & (X, 2) & (X, 3) & (X, 4) & (X, 5) \\ 1 & 1 & 1 & 1 & 1 \end{pmatrix} \quad (147)$$

which corresponds to the global conserved quantity X_n . In contrast, its kernel is empty denoting the absence of symmetries. Setting $-\beta k_1$ as “potential” field, y_p , the nonequilibrium potential reads

$$\phi_n = \beta k_1 X_n, \quad (148)$$

while the fundamental forces are equal to

$$\mathcal{F}_{(X, r)} = \beta (k_1 - k_r), \quad \text{for } r = 2, \dots, 5. \quad (149)$$

The trajectory EP can be thus expressed as

$$\Sigma[\mathbf{n}_t | \pi] = v[\mathbf{n}_t | \pi] + \sum_{r=2}^5 \sigma_r[\mathbf{n}_t | \pi] + \Delta\Phi[\mathbf{n}_t | \pi], \quad (150)$$

where

$$v[\mathbf{n}_t | \pi] := -\beta \int_{t_0}^t d\tau \partial_\tau [k_1(\tau) X_n(\tau)]|_{n=n_\tau} \quad (151a)$$

$$\sigma_r[\mathbf{n}_t | \pi] := -\beta \int_{t_0}^t d\tau [k_1(\tau) - k_r(\tau)] I_r(\tau). \quad (151b)$$

In order to show the emergence of a symmetry following a change of physical topology, let us now assume that $a_x = a_z = a$ and carry on the same analysis as before. The M -matrix now becomes,

$$M = (X, 1) \begin{pmatrix} 1 & 2 & 3 & 4 \\ a & -a & 0 & a \\ 0 & a & 0 & -a \\ 0 & 0 & -a & 0 \\ -a & 0 & 0 & 0 \\ 0 & 0 & a & 0 \end{pmatrix}. \quad (152)$$

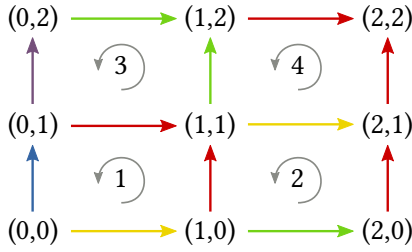


FIG. 10. Illustration of a 3×3 grid with nearest-neighbor transitions triggered by a reservoir chosen at random among five. The color of each transition corresponds to a different reservoir: 1, yellow; 2, green; 3, purple; 4, blue; and 5, red.

whose kernel and cokernel are one and two-dimensional, respectively. The symmetries are given by

$$\psi = \begin{pmatrix} 1 & 2 & 3 & 4 \\ 0 & 1 & 0 & 1 \end{pmatrix}, \quad (153)$$

and tell us that the second and fourth cycles are not physically independent, as they are coupled to the same reservoirs and all displacements are the same. The basis of $\text{coker } M$,

$$\ell^X = \begin{pmatrix} (X, 1) & (X, 2) & (X, 3) & (X, 4) & (X, 5) \\ 1 & 1 & 1 & 1 & 1 \end{pmatrix} \quad (154a)$$

$$\ell^V = \begin{pmatrix} (X, 1) & (X, 2) & (X, 3) & (X, 4) & (X, 5) \\ 0 & 0 & 1 & 0 & 1 \end{pmatrix} \quad (154b)$$

identifies two state variables, the first of which is the global conserved quantity, X_n , whereas the second is

$$V_n = \begin{pmatrix} (0, 0) & (1, 0) & (0, 1) & (2, 0) & (1, 1) & (0, 2) & (2, 1) & (1, 2) & (2, 2) \\ 0 & 0 & 0 & 0 & a & a & a & a & 2a \end{pmatrix} \quad (155)$$

whose interpretation is not obvious. It arises from the fact that x - and z -transitions are indistinguishable and the reservoirs 3 and 5 split the states into three groups, see Fig. 11, which are identified by different values of V_n , Eq. (155). We can set $(X, 1)$ and $(X, 3)$ as the reservoirs of the set $\{y_p\}$, according to which the Massieu potential of the state n reads

$$\phi_n = \beta [k_1 X_n + (k_3 - k_1) V_n]. \quad (156)$$

The number of fundamental forces is thus reduced,

$$\mathcal{F}_{(X, 2)} = \beta k_1 - \beta k_2, \quad (157a)$$

$$\mathcal{F}_{(X, 4)} = \beta k_1 - \beta k_4, \quad (157b)$$

$$\mathcal{F}_{(X, 5)} = \beta k_3 - \beta k_5. \quad (157c)$$

The EP can be easily written.

This model exemplifies the emergence of nontrivial conservation laws whose identification is not straightforward, and motivates the need for a systematic procedure capable of separating the conservative contributions to the EP from the nonconservative ones.

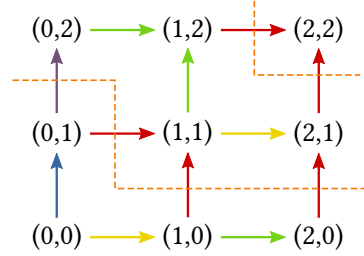


FIG. 11. Illustration of the randomized grid in Fig. 10 for $a_x = a_z = a$. The grid is split into three groups of states by the transitions corresponding to the third (purple) and fifth (red) reservoir: $\{(0, 0), (1, 0), (0, 1), (2, 0)\}$, $\{(1, 1), (0, 2), (2, 1), (1, 2)\}$, and $\{(2, 2)\}$.

VII. CONCLUSIONS AND PERSPECTIVES

The central achievement of this paper is to show that the EP of an open system described by stochastic thermodynamics is shaped by the way conserved quantities constrain the exchanges between the system and the reservoirs. Some of these conserved quantities are the obvious ones which do not depend on the system details (e.g. energy, particle number). But we provide a systematic procedure to identify the nontrivial ones which depend on the system topology. As a result, we can split the EP into three fundamental contributions, one solely caused by the time-dependent drivings, another expressed as the change of a nonequilibrium Massieu potential, and a third one which contains the fundamental set of flux and forces. Table III indicates which of these contributions play a role in different known processes. We also showed how to make use of this decomposition to derive a finite-time detailed FT solely expressed in terms of physical quantities, as well as to assess the cost of manipulating nonequilibrium states via time-dependent driving and nonconservative forces.

We believe that this work provides a comprehensive formulation of stochastic thermodynamics. Our framework can be systematically used to study any specific model (as we illustrated on several examples) and demonstrates the crucial importance of conservation laws in thermodynamics, at, as well as out of equilibrium.

ACKNOWLEDGMENTS

We thank G. Bulnes Cuetara for advises on the FT proof. This work was funded by the National Research Fund of Luxembourg (AFR PhD Grant 2014-2, No. 9114110) and the European Research Council (Project No. 681456).

Appendix A: Proof of the Fluctuation Relation

We now give the proof of the finite time detailed FTs (87) using moment generating functions. Alternatively, it can be proved using the approach developed in Ref. [48]. For our purposes, we change our notation for a bracket operatorial one.

Let $P_t(n, v, \{\sigma_{y_f}\})$ be the joint probability of observing a trajectory ending in the state n along which the driving contribution is v while the flow ones are $\{\sigma_{y_f}\}$. The above probabilities, one for each n , are stacked in the ket $|P_t(v, \{\sigma_{y_f}\})\rangle$. The time evolution of the moment generating function of the above probabilities,

$$|\Lambda_t(\xi_d, \{\xi_{y_f}\})\rangle := \int dv \prod_{y_f} d\sigma_{y_f} \exp \{-\xi_d v - \xi^{y_f} \sigma_{y_f}\} |P_t(v, \{\sigma_{y_f}\})\rangle, \quad (\text{A1})$$

is ruled by the biased stochastic dynamics

$$d_t |\Lambda_t(\xi_d, \{\xi_{y_f}\})\rangle = \mathcal{W}_t(\xi_d, \{\xi_{y_f}\}) |\Lambda_t(\xi_d, \{\xi_{y_f}\})\rangle, \quad (\text{A2})$$

where the entries of the biased generator are given by

$$\begin{aligned} \mathcal{W}_{nm,t}(\xi_d, \{\xi_{y_f}\}) &= \begin{cases} \sum_v w_{nm}^v \exp \{\xi^{y_f} \mathcal{F}_{y_f} Y_{y_f, (nm, v)}\} & \text{if } n \neq m \\ \sum_v \sum_{n'} w_{n'm}^v + \xi_d \partial_t \phi_m & \text{if } n = m \end{cases}. \end{aligned} \quad (\text{A3})$$

Because of the local detailed balance (24), the stochastic generator satisfies the following symmetry

$$\mathcal{W}_t^T(\xi_d, \{\xi_{y_f}\}) = \mathcal{B}_t^{-1} \mathcal{W}_t(\xi_d, \{1 - \xi_{y_f}\}) \mathcal{B}_t, \quad (\text{A4})$$

where the entries of \mathcal{B}_t are given by

$$\mathcal{B}_{nm,t} := \exp \{\phi_n\} \delta_{m,n}. \quad (\text{A5})$$

Also, the initial condition is given by the equilibrium distribution (48), which reads

$$|\Lambda_0(\xi_d, \{\xi_{y_f}\})\rangle = |p_{\text{eq}_i}\rangle = \mathcal{B}_0/Z_0 |1\rangle, \quad (\text{A6})$$

From Eqs. (A8), (A9) and (A10) we deduce that

$$\mathcal{X}_t^{-1} \mathcal{U}_t(\xi) \mathcal{X}_0 = \mathcal{T}_+ \exp \left\{ \int_0^t d\tau \left[d_\tau \mathcal{X}_\tau^{-1} \mathcal{X}_\tau + \mathcal{X}_\tau^{-1} \mathcal{W}_\tau(\xi) \mathcal{X}_\tau \right] \right\}. \quad (\text{A11})$$

We can now come back to our specific biased stochastic dynamics (A2). The moment generating function of $P_t(v, \{\sigma_{y_f}\})$ is thus given by

$$\Lambda_t(\xi_d, \{\xi_{y_f}\}) = \langle 1 | \Lambda_t(\xi_d, \{\xi_{y_f}\}) \rangle = \langle 1 | \mathcal{U}_t(\xi_d, \{\xi_{y_f}\}) \mathcal{B}_0/Z_0 | 1 \rangle = \langle 1 | \frac{\mathcal{B}_t}{Z_t} \mathcal{B}_t^{-1} \mathcal{U}_t(\xi_d, \{\xi_{y_f}\}) \mathcal{B}_0 | 1 \rangle \frac{Z_t}{Z_0}, \quad (\text{A12})$$

where $\mathcal{U}_t(\xi_d, \{\xi_{y_f}\})$ is the time-evolution operator of the biased stochastic dynamics (A2). From the condition 2 discussed in the main text, it follows that $\langle 1 | \mathcal{B}_t/Z_t$ with $Z_t := \exp\{\Phi_{\text{eq}_i}\}$ is the equilibrium initial distribution of the backward process $\langle p_{\text{eq}_f} |$. Using the relation in Eq. (A11), the above term can be rewritten as

$$= \langle p_{\text{eq}_f} | \mathcal{T}_+ \exp \left\{ \int_0^t d\tau \left[\partial_\tau \mathcal{B}_\tau^{-1} \mathcal{B}_\tau + \mathcal{B}_\tau^{-1} \mathcal{W}_\tau(\xi_d, \{\xi_{y_f}\}) \mathcal{B}_\tau \right] \right\} | 1 \rangle \exp \{ \Delta \Phi_{\text{eq}} \}, \quad (\text{A13})$$

where $\Delta \Phi_{\text{eq}} \equiv \ln Z_t/Z_0$. Since $\partial_\tau \mathcal{B}_\tau^{-1} \mathcal{B}_\tau = \text{diag} \{-\partial_t \phi_n\}$ the first term in square bracket can be added to the diagonal entries of the second term, thus giving

$$= \langle p_{\text{eq}_f} | \mathcal{T}_+ \exp \left\{ \int_0^t d\tau \left[\mathcal{B}_\tau^{-1} \mathcal{W}_\tau(\xi_d - 1, \{\xi_{y_f}\}) \mathcal{B}_\tau \right] \right\} | 1 \rangle \exp \{ \Delta \Phi_{\text{eq}} \}. \quad (\text{A14})$$

where $Z_0 := \exp\{\Phi_{\text{eq}_i}\}$ is the partition function. The ket $|1\rangle$ refers to the vector in the state space whose entries are all equal to one.

In order to proceed further, it is convenient to first prove a preliminary result. Let us consider the generic biased dynamics, e.g. Eq. (A2),

$$d_t |\Lambda_t(\xi)\rangle = \mathcal{W}_t(\xi) |\Lambda_t(\xi)\rangle, \quad (\text{A7})$$

whose initial condition is $|\Lambda_0(\xi)\rangle = |p(0)\rangle$. A formal solution of Eq. (A7) is $|\Lambda_t(\xi)\rangle = \mathcal{U}_t(\xi) |p(0)\rangle$, where the time-evolution operator reads $\mathcal{U}_t(\xi) = \mathcal{T}_+ \exp \left\{ \int_0^t d\tau \mathcal{W}_\tau(\xi) \right\}$, \mathcal{T}_+ being the time-ordering operator. We clearly have $d_t \mathcal{U}_t(\xi) = \mathcal{W}_t(\xi) \mathcal{U}_t(\xi)$. Let us now consider the following transformed evolution operator

$$\tilde{\mathcal{U}}_t(\xi) := \mathcal{X}_t^{-1} \mathcal{U}_t(\xi) \mathcal{X}_0, \quad (\text{A8})$$

\mathcal{X}_t being a generic invertible operator. Its dynamics is ruled by the following biased stochastic dynamics

$$\begin{aligned} d_t \tilde{\mathcal{U}}_t(\xi) &= d_t \mathcal{X}_t^{-1} \mathcal{U}_t(\xi) \mathcal{X}_0 + \mathcal{X}_t^{-1} d_t \mathcal{U}_t(\xi) \mathcal{X}_0 \\ &= \{d_t \mathcal{X}_t^{-1} \mathcal{X}_t + \mathcal{X}_t^{-1} \mathcal{W}_t(\xi) \mathcal{X}_t\} \tilde{\mathcal{U}}_t(\xi) \\ &\equiv \tilde{\mathcal{W}}_t(\xi) \tilde{\mathcal{U}}_t(\xi), \end{aligned} \quad (\text{A9})$$

which allows us to conclude that the transformed time-evolution operator is given by

$$\tilde{\mathcal{U}}(\xi) = \mathcal{T}_+ \exp \left\{ \int_0^t d\tau \tilde{\mathcal{W}}_\tau(\xi) \right\}. \quad (\text{A10})$$

The symmetry (A4) and the condition 2 allow us to recast the latter into

$$= \langle p_{\text{eq}_f} | \mathcal{T}_+ \exp \left\{ \int_0^t d\tau \mathcal{W}_\tau^T (\xi_d - 1, \{1 - \xi_{y_f}\}) \right\} | 1 \rangle \exp \{ \Delta \Phi_{\text{eq}} \} . \quad (\text{A15})$$

The crucial step comes as we transform the integration variable from τ to $\tau^\dagger = t - \tau$. Accordingly, the time-ordering operator, \mathcal{T}_+ , becomes an anti-time-ordering one \mathcal{T}_- , while the biased generator, Eq. (A3), becomes

$$\begin{aligned} \mathcal{W}_{nm, t-\tau^\dagger}(\xi_d, \{\xi_{y_f}\}) &= \begin{cases} \sum_v w_{nm}^v(t - \tau^\dagger) \exp \{ \xi^{y_f} \mathcal{F}_{y_f}(t - \tau^\dagger) Y_{y_f, (nm, v)}(t - \tau^\dagger) \} & \text{if } n \neq m \\ \sum_v \sum_{n'} w_{n'm}^v(t - \tau^\dagger) + \xi_d \partial_{(t-\tau^\dagger)} [\phi_m(t - \tau^\dagger)] & \text{if } n = m \end{cases} \\ &= \begin{cases} \sum_v w_{nm}^v(t - \tau^\dagger) \exp \{ \xi^{y_f} \mathcal{F}_{y_f}(t - \tau^\dagger) Y_{y_f, (nm, v)}(t - \tau^\dagger) \} & \text{if } n \neq m \\ \sum_v \sum_{n'} w_{n'm}^v(t - \tau^\dagger) - \xi_d \partial_{\tau^\dagger} [\phi_m(t - \tau^\dagger)] & \text{if } n = m \end{cases} \\ &= \mathcal{W}_{nm, t-\tau^\dagger}(-\xi_d, \{\xi_{y_f}\}) \equiv \mathcal{W}_{nm, \tau^\dagger}^\dagger(-\xi_d, \{\xi_{y_f}\}). \end{aligned} \quad (\text{A16})$$

In the last definition, the dagger is understood as a time-reversing operator, so that $\mathcal{W}_{\tau^\dagger}^\dagger(\xi_d, \{\xi_{y_f}\})$ becomes the biased generator of the dynamics subject to time-reversed protocol, π^\dagger , i.e. the dynamics of the backward process. Equation (A15) thus becomes

$$= \langle p_{\text{eq}_f} | \mathcal{T}_- \exp \left\{ \int_0^t d\tau^\dagger \mathcal{W}_{\tau^\dagger}^T (1 - \xi_d, \{1 - \xi_{y_f}\}) \right\} | 1 \rangle \exp \{ \Delta \Phi_{\text{eq}} \} . \quad (\text{A17})$$

Upon a global transposition, we can write

$$= \langle 1 | \mathcal{T}_- \exp \left\{ \int_0^t d\tau^\dagger \mathcal{W}_{\tau^\dagger}^\dagger (1 - \xi_d, \{1 - \xi_{y_f}\}) \right\} | p_{\text{eq}_f} \rangle \exp \{ \Delta \Phi_{\text{eq}} \} , \quad (\text{A18})$$

where we also used the relationship between transposition and time-ordering

$$\mathcal{T}_+ \left(\prod_i A_{t_i}^T \right) = (\mathcal{T}_- \prod_i A_{t_i})^T , \quad (\text{A19})$$

in which A_t is a generic operator. From the last expression, we readily obtain

$$\begin{aligned} &= \langle 1 | \mathcal{U}_t^\dagger (1 - \xi_d, \{1 - \xi_{y_f}\}) | p_{\text{eq}_f} \rangle \exp \{ \Delta \Phi_{\text{eq}} \} \\ &= \Lambda_t^\dagger (1 - \xi_d, \{1 - \xi_{y_f}\}) \exp \{ \Delta \Phi_{\text{eq}} \} , \end{aligned} \quad (\text{A20})$$

where $\Lambda_t^\dagger(\xi_d, \{\xi_{y_f}\})$ is the moment generating function of $P_t^\dagger(v, \{\sigma_{y_f}\})$. Summarizing, we have the following symmetry

$$\Lambda_t(\xi_d, \{\xi_{y_f}\}) = \Lambda_t^\dagger (1 - \xi_d, \{1 - \xi_{y_f}\}) \exp \{ \Delta \Phi_{\text{eq}} \} , \quad (\text{A21})$$

whose inverse Laplace transform gives the FT

$$\frac{P_t(v, \{\sigma_{y_f}\})}{P_t^\dagger(-v, \{-\sigma_{y_f}\})} = \exp \{ v + \sum_{y_f} \sigma_{y_f} + \Delta \Phi_{\text{eq}} \} . \quad (\text{A22})$$

Fundamental Cycles

The finite-time detailed FT for flow contributions along fundamental cycles, Eq. (94), follows the same logic and mathematical steps described above. The moment generating function which now must be taken into account is

$$|\Lambda_t(\xi_d, \{\xi_\eta\})\rangle := \int dv \prod_\eta d\gamma_\eta \exp \{ -\xi_d v - \xi^\eta \gamma_\eta \} |P_t(v, \{\gamma_\eta\})\rangle , \quad (\text{A23})$$

which is ruled by the biased generator whose entries are

$$\begin{aligned} &\mathcal{W}_{nm, t}(\xi_d, \{\xi_\eta\}) \\ &= \begin{cases} \sum_v w_{nm}^v \exp \{ -\xi^\eta \mathcal{A}_\eta \zeta_{\eta, (nm, v)} \} & \text{if } n \neq m \\ \sum_v \sum_{n'} w_{n'm}^v + \xi_d \partial_t \phi_m & \text{if } n = m \end{cases} . \end{aligned} \quad (\text{A24})$$

The symmetry of the latter generator—on top of which the proof is constructed—is based on the expression of the local detailed balance given in Eq. (24),

$$\mathcal{W}_t^T(\xi_d, \{\xi_\eta\}) = \mathcal{B}_t^{-1} \mathcal{W}_t(\xi_d, \{1 - \xi_\eta\}) \mathcal{B}_t , \quad (\text{A25})$$

where the entries of \mathcal{B}_t are given in Eq. (A5). Following the steps from Eq. (A12) to Eq. (A21), with the above definitions and equalities, Eqs. (A23)–(A25), proves the FT in Eq. (94).

[1] K. Sekimoto, *Stochastic Energetics*, 1st ed., Lecture Notes in Physics, Vol. 799 (Springer-Verlag Berlin Heidelberg, 2010).

[2] C. Jarzynski, *Annu. Rev. Condens. Matter Phys.* **2**, 329 (2011).

[3] U. Seifert, *Rep. Prog. Phys.* **75**, 126001 (2012).

[4] C. Van den Broeck and M. Esposito, *Physica A* **418**, 6 (2015).

[5] S. Ciliberto, *Phys. Rev. X* **7**, 021051 (2017).

[6] G. Verley, T. Willaert, C. Van den Broeck, and M. Esposito, *Phys. Rev. E* **90**, 052145 (2014).

[7] K. Proesmans, Y. Dreher, M. c. v. Gavrilov, J. Bechhoefer, and C. Van den Broeck, *Phys. Rev. X* **6**, 041010 (2016).

[8] A. Berut, A. Arakelyan, A. Petrosyan, S. Ciliberto, R. Dillenschneider, and E. Lutz, *Nature* **483**, 187 (2012).

[9] J. M. Horowitz and M. Esposito, *Phys. Rev. X* **4**, 031015 (2014).

[10] Y. Jun, M. Gavrilov, and J. Bechhoefer, *Phys. Rev. Lett.* **113**, 190601 (2014).

[11] J. M. R. Parrondo, J. M. Horowitz, and T. Sagawa, *Nature Phys.* **11**, 131 (2015).

[12] T. E. Ouldridge, C. C. Govern, and P. R. ten Wolde, *Phys. Rev. X* **7**, 021004 (2017).

[13] R. Rao and L. Peliti, *J. Stat. Mech. Theor. Exp.*, Po6001 (2015).

[14] A. C. Barato and U. Seifert, *Phys. Rev. X* **6**, 041053 (2016).

[15] M. Esposito, *Phys. Rev. E* **85**, 041125 (2012).

[16] M. Polettini, G. Bulnes Cuetara, and M. Esposito, *Phys. Rev. E* **94**, 052117 (2016).

[17] G. Bulnes Cuetara, M. Esposito, and A. Imparato, *Phys. Rev. E* **89**, 052119 (2014).

[18] H.-H. Hasegawa, J. Ishikawa, K. Takara, and D. Driebe, *Phys. Lett. A* **374**, 1001 (2010).

[19] K. Takara, H.-H. Hasegawa, and D. Driebe, *Phys. Lett. A* **375**, 88 (2010).

[20] M. Esposito and C. Van den Broeck, *Europhys. Lett.* **95**, 40004 (2011).

[21] H. Callen, *Thermodynamics and an Introduction to Thermostatistics* (Wiley, 1985).

[22] D. A. Beard and H. Qian, *Chemical Biophysics. Quantitative Analysis of Cellular Systems* (Cambridge University Press, 2008), § 1.7.2.

[23] B. Rutten, M. Esposito, and B. Cleuren, *Phys. Rev. B* **80**, 235122 (2009).

[24] P. Strasberg, G. Schaller, T. Brandes, and M. Esposito, *Phys. Rev. Lett.* **110**, 040601 (2013).

[25] The definition of $\{\mathbf{L}^\lambda\}$ can be further clarified using a graph-theoretical argument. Let us notice that from Eq. (12) one concludes that $\mathbf{\ell}^\lambda Y \in (\ker D)^\perp$, for all λ . Since $(\ker D)^\perp = \text{im } D^T$ and D^T provides a mapping from $\{n\}$ to $\{e\}$ —up to a constant—[49], one can implicitly map the vectors $\{\mathbf{\ell}^\lambda Y\}$ into states-space vectors $\{\mathbf{L}^\lambda\}$ via $D^T \mathbf{L}^\lambda = \mathbf{\ell}^\lambda Y$, i.e. Eq. (13).

[26] One may argue that the above statement might be due the fact that we fixed the electron occupancy of each QD to one, Eq. (7). However, the same conclusion is reached when assuming: $N_{00} = 0$, $N_{01} = v_d$, $N_{10} = v_u$, and $N_{11} = v_u + v_d$, for some positive integer values v_u and v_d .

[27] By hypothesis the matrix whose entries are $\{M_\eta^y\}$ has maximal rank N_η . From the definition of conservation law $\ell_{y_f}^\lambda M_\alpha^{y_f} = -\ell_{y_p}^\lambda M_\alpha^{y_p} \neq 0$, where last inequality follows from the fact that we chose the matrix whose entries are $\{\ell_{y_p}^\lambda\}$ to have maximal rank. Let us now assume by contradiction that $\{M_\eta^y\}$ is singular, and let us denote by $\{x^\eta\}$ a vector of $\text{coker } M$. We can thus construct a vector $\{x^\alpha\}$ having as entries corresponding to η , $\{x^\eta\}$, and zero for the others, so that $M_\alpha^{y_f} x^\alpha = 0$, $\forall y_f$. From the equation above we obtain that $\ell_{y_p}^\lambda M_\alpha^{y_p} x^\alpha = -\ell_{y_f}^\lambda M_\alpha^{y_f} x^\alpha = 0$. Since $\{\ell_{y_p}^\lambda\}$ is nonsingular we must conclude that $M_\alpha^{y_p} x^\alpha = 0$, $\forall y_p$, and thus $M_\alpha^y x^\alpha = 0$, $\forall y$, in contradiction with the first hypothesis.

[28] J. Schnakenberg, *Rev. Mod. Phys.* **48**, 571 (1976).

[29] A. Kolmogoroff, *Math. Ann.* **112**, 155 (1936).

[30] F. P. Kelly, *Reversibility and Stochastic Networks* (John Wiley & Sons Ltd., 1979).

[31] E. T. Jaynes, *Phys. Rev.* **106**, 620 (1957).

[32] L. Peliti, *Statistical Mechanics in a Nutshell* (Princeton University Press, 2011), § 3.17.

[33] U. Seifert, *Phys. Rev. Lett.* **95**, 040602 (2005).

[34] M. Polettini, *Europhys. Lett.* **97**, 30003 (2012).

[35] A. Wachtel, J. Vollmer, and B. Altaner, *Phys. Rev. E* **92**, 042132 (2015).

[36] M. Campisi, P. Hänggi, and P. Talkner, *Rev. Mod. Phys.* **83**, 771 (2011).

[37] M. Polettini, *Lett. Math. Phys.* **105**, 89 (2014).

[38] C. Jarzynski, *Phys. Rev. Lett.* **78**, 2690 (1997).

[39] G. E. Crooks, *J. Stat. Phys.* **90**, 1481 (1998).

[40] M. Polettini and M. Esposito, *J. Stat. Mech. Theor. Exp.* **2014**, P10033 (2014).

[41] D. Andrieux and P. Gaspard, *J. Stat. Phys.* **127**, 107 (2007).

[42] B. Altaner, .

[43] G. Bulnes Cuetara and M. Esposito, *New J. Phys.* **17**, 095005 (2015).

[44] S. Liepelt and R. Lipowsky, *Phys. Rev. Lett.* **98**, 258102 (2007).

[45] B. Altaner, A. Wachtel, and J. Vollmer, *Phys. Rev. E* **92**, 042133 (2015).

[46] U. Seifert, *Eur. Phys. J. E* **34**, 26 (2011).

[47] J. M. Horowitz and M. Esposito, *Phys. Rev. E* **94**, 020102 (2016).

[48] R. García-García, D. Domínguez, V. Lecomte, and A. B. Kolton, *Phys. Rev. E* **82**, 030104 (2010).

[49] U. Knauer, *Algebraic graph theory: morphisms, monoids and matrices*, Vol. 41 (Walter de Gruyter, 2011), § 6.2.